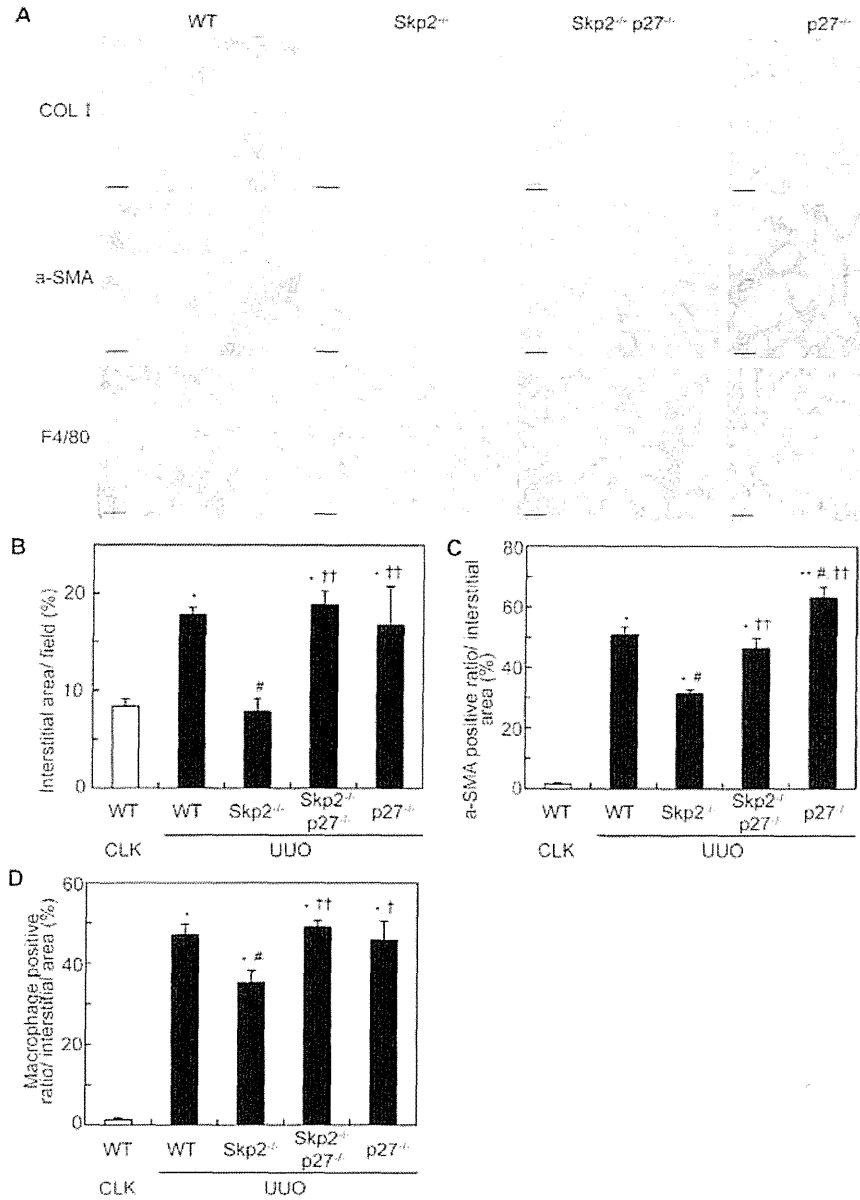

Figure 5. Levels of tubulointerstitial fibrotic lesions. (**A**) Representative images of UUO kidney sections in WT, Skp2$^{-/-}$, Skp2$^{-/-}$p27$^{-/-}$ and p27$^{-/-}$ mice immunostained for type I collagen (top panels), α-SMA (middle panels) and F4/80 (bottom panels) at 7 days after UUO, scale bars: 50 μm. (**B**) The ratios of the interstitial area in the UUO kidneys were quantified using the sections stained for type I collagen. (**C, D**) The intensities of the α-SMA (**C**) and F4/80 (**D**) immunostaining were quantified using Scion Image software. The CLK kidneys in WT mice were evaluated as controls. *P<0.01 versus WT CLK kidneys, $^{\#}P$<0.01 versus WT UUO kidneys and $^{\dagger}P$<0.05, $^{\dagger\dagger}P$<0.01 versus Skp2$^{-/-}$ UUO kidneys.
doi:10.1371/journal.pone.0036249.g005

aggravated, by the additional p27-deficiency in Skp2$^{-/-}$p27$^{-/-}$ double-knockout mice, and 3) the aggravation of UUO renal injury was also noted in p27$^{-/-}$ mice. These findings suggest that the decrease in p27 targeted by Skp2 is involved in the progression of UUO renal injury.

No significant renal accumulation of p57, p130, TOB1, cyclin A or cyclin D1, which are also Skp2 targets, was observed, suggesting that these proteins are not targets for Skp2 in UUO renal injury. In contrast, increases in several other possible Skp2 targets, including p21, c-Myc, b-Myb and cyclin E, were also observed in the ameliorated UUO kidneys in Skp2$^{-/-}$ mice, but showed slight increments compared with p27 accumulation. Because c-Myc, b-Myb and cyclin E accelerate the cell cycle and stimulate cell proliferation, it is unlikely that their increases are involved in the suppression of tubular and interstitial cell proliferation in UUO renal injury in Skp2$^{-/-}$ mice. However, the role of the moderately increased p21, another CDKI possibly targeted by Skp2, in the suppression of UUO renal injury in Skp2$^{-/-}$ mice remains to be clarified. Since it has been reported that p21 regulates interstitial cells in UUO kidneys [23], the decrease in p21 targeted by Skp2 may be involved in the progression of interstitial cell proliferation in UUO kidneys. Further studies using Skp2$^{-/-}$p21$^{-/-}$ double-

knockout mice are needed to clarify the role of p21 in UUO renal injury.

p27 deletion not only abolished the protective effects of Skp2$^{-/-}$ genotype, but also makes the renal lesion worse compared to the wild type. p27 deletion may promote unscheduled activations of various cyclin-dependent kinases. Thereby renal epithelial cell growth and following tubular dilation induced by renal obstruction may be irregularly enhanced in p27$^{-/-}$ mice. In the Skp2$^{-/-}$ (Figure 1) and Skp2$^{-/-}$p27$^{-/-}$ mice (data not shown), another Skp2 targets such as p21 and c-Myc are accumulated. c-Myc plays roles for promotion of cell growth and apoptosis, whereas p27 and p21 are negative regulators in cell proliferation. The increased c-Myc may play opposite roles against p27 and p21 for tubular epithelial cell proliferation. Moreover, it has been reported that p21 inhibits c-Myc expression [31]. c-Myc promotes Skp2-mediated degradation of p27 [32]. Therefore, Skp2 target cell cycle regulators are functionally related each other. Skp2 deletion may induce these unbalances of cell cycle regulators not only directly but also indirectly, thereby the cell proliferation and apoptosis were abrogated in the UUO kidney.

In addition to the diminished amelioration of tubular and interstitial cell proliferation, aggravation of interstitial fibrosis composed of increased deposition of type I collagen, interstitial expression of α-SMA, and infiltration of macrophages was noted in the UUO kidneys in Skp2$^{-/-}$p27$^{-/-}$ and p27$^{-/-}$ mice. These findings suggest that the regulation of p27 by Skp2 is involved in the development of tubulointerstitial fibrosis. It has been reported that type II epithelial-mesenchymal transdifferentiation (EMT) occurs in progressive nephropathies to differentiate myofibroblasts from renal epithelial cells [33]. The expression levels of α-SMA, fibronectin and vimentin are closely associated with type II EMT as typical markers for myofibroblasts [33–36]. Our data suggest that the Skp2/p27 pathway may contribute to EMT in progressive UUO renal injury, although further studies are required.

Talking all our findings into consideration, it is suggested that degradation of p27 targeted by Skp2 accelerated the progression of renal tubular epithelial cell proliferation, tubular dilation and tubulointerstitial fibrosis in UUO renal injury. Therefore, we conclude that p27 is a main target for Skp2 and that degradation of p27 by Skp2 is required for the progression of renal injury mediated by UUO. Based on this, inhibitors of SCF-Skp2/Cks1 E3 ligase that specifically promote p27 degradation may be effective for the treatment of progressive nephropathy. Further studies are required to examine this possibility.

Methods

Experimental animals

The generation of Skp2$^{-/-}$ mice [13] and p27$^{-/-}$ mice [37] were signed by Nakayama et al. To obtain WT [Skp2$^{+/+}$p27$^{+/+}$], Skp2$^{-/-}$, Skp2$^{-/-}$p27$^{-/-}$ and p27$^{-/-}$ offspring, heterozygous Skp2$^{+/-}$p27$^{+/-}$ mice were mated. The mice included in this study were 6-week-old male mice weighing 20–25 g. The mice were allowed free access to food and water, and were maintained under a 12-h/12-h light-dark cycle. We confirmed the WT and disrupted alleles of Skp2 and p27 by PCR. The mice were treated according to protocols approved by the Hamamatsu University School of Medicine Animal Care Committees at the Center Animal Care facility.

Experimental design

Ureteral obstruction was achieved by ligating the left ureter with 3-0 silk through a left lateral incision. WT, Skp2$^{-/-}$, Skp2$^{-/-}$p27$^{-/-}$ and p27$^{-/-}$ mice (n = 4–5 per group) were sacrificed at 7 days after the operation. The obstructed (UUO) and non-obstructed contralateral (CLK) kidneys were harvested from each mouse and subjected to the analyses described below. The experimental protocol was approved by the Ethics Review Committee for Animal Experimentation of Hamamatsu University School of Medicine.

Immunoblot analysis

Whole kidney tissues were dissolved in RIPA buffer (25 mmol/L Tris-HCl pH 7.4, 150 mmol/L NaCl, 0.1% SDS, 0.5% Triton-X100, 0.5% sodium deoxycholate) containing protease inhibitors (150 mg/ml PMSF, 5 mg/ml aprotinin, 5 mg/ml pepstatin, 5 mg/ml leupeptin, 5 mg/ml E-64) at 4°C. After incubation for 30 min, the lysates were centrifuged at 13000×*g* for 15 min at 4°C. The protein concentrations of the lysates were measured using a protein assay reagent (Bio-Rad Laboratories, Hercules, CA). Soluble lysates were boiled with 4×SDS sample buffer (250 mmol/L Tris-HCl pH 6.8, 12% SDS, 40% glycerol, 20% 2-mercaptoethanol, 1% bromophenol blue) for 3 min. Equal amounts of proteins were loaded and separated by SDS-PAGE. The separated proteins were transferred to polyvinylidene difluoride membranes, followed by immunoblotting with the following antibodies: mouse monoclonal anti-p27 and anti-p130 (BD Transduction Laboratories, San Jose, CA); anti-p21 (Santa Cruz Biotechnology, Santa Cruz, CA); anti-Myc (Cell Signaling Technology, Danvers, MA); anti-α-tubulin (Sigma, St. Louis, MO); rabbit monoclonal anti-p57 (Abcam, Cambridge, UK); rabbit polyclonal anti-TOB (Abcam); anti-b-Myb, anti-cyclin A, anti-cyclin D1 and anti-cyclin E (Santa Cruz Biotechnology). α-tubulin was evaluated as an internal control. The antibody-bound proteins were visualized using an enhanced chemiluminescence system (Perkin Elmer, Wellesley, MA).

Histopathological and immunohistochemical analyses

Kidney tissues were fixed in 4% paraformaldehyde in PBS and embedded in paraffin. Tissue sections (3-μm thickness) were rehydrated and subjected to Masson's trichrome staining for histopathological analysis. The levels of fibrotic tubulointerstitial lesions were graded semiquantitatively as follows: 0, absent (0%); 1, weak (≤10%); 2, mild (>10 to ≤30%); 3, moderate (>30 to ≤50%); 4, strong (>50%) in twenty randomly selected non-overlapping renal cortical fields at ×400 magnification. The percentage of dilated tubules per total tubules, the number of renal tubular epithelial cells in a tubule which was obtained as the number of tubular epithelial cells divided by the number of tubules, and the number of interstitial cells were counted in 10 randomly selected non-overlapping renal cortical fields at ×400 magnification. The immunoreactivities for Ki67, type I collagen, α-smooth muscle actin (α-SMA) and F4/80, a marker protein for macrophages, were determined using a Histofine SAB-PO kit (Nichirei, Tokyo, Japan) as a standard biotin-streptavidin-peroxidase method as described previously [24]. The primary antibodies were as follows: rabbit polyclonal anti-human Ki67 (Novocastra Laboratories, Newcastle-upon-Tyne, UK); anti-mouse type I collagen (Abcam); mouse monoclonal anti-human α-SMA (DAKO, Hamburg, Germany); and rat anti-mouse F4/80 (Serotec, Oxford, UK). The secondary antibodies were affinity-purified biotinylated goat anti-mouse or anti-rabbit immunoglobulin, and peroxidase-conjugated anti-rat immunoglobulin (Nichirei, Tokyo, Japan). The kidney sections were lightly counterstained with hematoxylin. The numbers of Ki67-positive tubular epithelial and interstitial cells were counted in 10 randomly selected non-overlapping renal cortical fields at ×400 magnification and the mean values were obtained. The type I collagen-

positive interstitial area and the areas positive for α-SMA and F4/80 were quantified in 10 randomly selected non-overlapping fields at ×400 magnification using Scion Image software (Scion Corp., Frederick, MD). We set a threshold to automatically compute the positive areas for each stain and computed the ratio of the positive areas to the whole interstitial area.

Evaluation of apoptosis

Deoxynucleotidyl transferase-mediated dUTP nick end labeling (TUNEL) was performed to detect apoptotic cell death using an ApopTag Plus Peroxidase *In Situ* Apoptosis Detection Kit (Chemicon, Temecula, CA). For each kidney, the number of apoptotic tubular epithelial and interstitial cells in 10 non-overlapping renal cortical fields was counted under ×400 magnification. The number of TUNEL-positive nuclei was averaged for each field.

Statistical analysis

Statistical analysis was performed using computer-assisted software (StatView 5.0; SAS Institute Inc.). All values are given as means ± SEM. Differences between groups were examined for statistical significance by analysis of variance. When a significant difference was found between two groups, a further statistical analysis was performed using the Bonferroni–Dunn test. Values of $P<0.05$ were considered to indicate statistical significance.

Supporting Information

Figure S1 The expression of Skp2 and/or p27 in WT, Skp2$^{-/-}$, Skp2$^{-/-}$p27$^{-/-}$ and p27$^{-/-}$ mice. The genotypes of the WT, Skp2$^{-/-}$, Skp2$^{-/-}$p27$^{-/-}$ and p27$^{-/-}$ mice were confirmed by PCR (**A**). The PCR primer sequences of Skp2 were sense 5′-CAGACCCTGACGCACCTCACG-3′ and antisense 5′-TTCTGACGCCCCGTTGCCTGCT-3′for WT, 5′-GGTGGATGTGGAATGTGTGCGAGGC-3′ for knockout allele; and of p27 were sense 5′-CGTGGGGTGTAGAATACTCCTTGT-3′ and antisense 5′-GATACGACCGTCCCTATCCTTTG-3′ for WT, 5′-TGCTAAAGCGCATGCTCCAGACTG-3′ for KO. Primers for glyceraldehyde-3-phosphate dehydrogenase (GAPDH), used as an internal control, were sense 5′-TGCACCACCAACTGCTTAG-3′ and antisense 5′-GATGCAGGGATGATGTTC-3′. The protein level of p27 in CLK (C) and UUO (U) kidneys in each genotype mouse (**B**). α-tubulin was used an internal control.
(TIF)

Figure S2 mRNA expression of UUO renal injury. mRNA level of COL I (**A**), α-SMA (**B**), F4/80 (**C**) and Fibronectin (**D**) measured by quantitative RT-PCR from CLK in WT mouse, and UUO kidneys in WT, Skp2$^{-/-}$, Skp2$^{-/-}$p27$^{-/-}$ and p27$^{-/-}$ mice. Total RNA was extracted from whole kidney tissue using the Isogen (Wako, Osaka, Japan) according to the manufacturer's instructions. Reverse transcription of the RNA was performed using the SuperScript First-Strand Synthsis System for RT-PCR kit (Invitrogen, Carlsbad, CA) with 2.5 μg of total RNA. The resulting cDNA was subjected to real-time PCR using the Roter-Gene 3000 System (Corbett Research, Mortlake, Australia) for amplification and online quantification. All PCR experiments were performed using a QuantiTect SYBR Green PCR kit purchased from TAKARA (TAKARA, Shiga, Japan). The PCR-primer sequences for COL I were sense 5′-AGAGCATGACCGATGGATTCC-3′ and antisense 5′-TTGCCAGTCTGCTGGTCCATG-3′ for α-SMA were sense 5′- ACTGGGACGACATGGAAAAG-3′ and antisense 5′-CATCTCCAGAGTCCAGCACA-3′: for F4/80 were sense 5′-GATGGGGGATGACCACACTT -3′ and antisense 5′-TTCAGGGCAAACGTCTCG-3′: for Fibronectin were sense 5′-ACGGTTTCCCATTACGCCAT-3′ and antisense 5′-CTTTCCATTCCCGAGGCAT-3′. GAPDH was evaluated as an internal control. The amount of COL I, α-SMA, F4/80 and Fibronectin mRNA was normalized for GAPDH mRNA in each sample. The CLK kidneys in WT mice were evaluated as controls. $^{*}P<0.05$, $^{**}P<0.005$ versus WT CLK kidneys, $^{\#}P<0.05$ versus WT UUO and $^{\dagger}P<0.05$ versus Skp2$^{-/-}$ UUO.
(TIF)

Figure S3 The immunoreactivity for Vimentin in UUO kidneys. Representitive images of immunohistochemical staining for Vimentin from WT CLK and UUO kidneys in each genotype mouse. The primary antibody was rabbit polyclonal anti-human Vimentin (Santa Cruz), scale bars: 50 μm.
(TIF)

Acknowledgments

We thank Dr. Hayato Ihara and our laboratory members for helpful discussions.

Author Contributions

Conceived and designed the experiments: SS TY KK AT. Performed the experiments: SS HF TM. Analyzed the data: NO KK NL HN TY MK. Contributed reagents/materials/analysis tools: KN KIN YK. Wrote the paper: SS TY MK.

References

1. Morgan DO (1995) Principles of CDK regulation. Nature 374: 131–134.
2. Sherr CJ, Roberts JM (1995) Inhibitors of mammalian G1 cyclin-dependent kinases. Gene & Dev 9: 1149–1163.
3. Nourse J, Firpo E, Flanagan WM, Coats S, Polyak K, et al. (1994) Interlukin-2-mediated elimination of the p27^{Kip1} cyclin-dependent kinases inhibitor prevented by rapamycin. Nature 372: 570–573.
4. Polyak K, Lee MH, Erdjument-Bromage H, Koff A, Roberts JM, et al. (1994) Cloning of p27^{Kip1}, a cyclin-dependent kinases inhibitor and potential mediator of extracellular antimitogenic signals. Cell 78: 59–66.
5. Coats S, Flanagan WM, Nourse J, Roberts JM (1996) Requirement of p27^{Kip1} for restriction point control of the fibroblast cell cycle. Science 272: 877–880.
6. Shankland SJ, Pippin J, Flanagan M, Coats SR, Nangaku M, et al. (1997) Mesangial cell proliferation mediated by PDGF and bFGF is determined by levels of the cyclin kinase inhibitor p27^{Kip1}. Kidney Int 51: 1088–1099.
7. Kamb A (1995) Cell-cycle refulators and cancer. Trends Genet 11: 136–140.
8. Weinberg RA (1995) The retinoblastoma protein and cell cycle control. Cell 81: 323–330.
9. Weissman AM (1997) Regulating protein degradation by ubiquitination. Immunol. Today 18: 189–198.
10. Hershko A, Ciechanover A (1998) The ubiquitin system. Annu Rev Biochem 67: 425–479.
11. Carrano AC, Eytan E, Hershko A, Pagano M (1999) SKP2 is required for ubiquitin-mediated degradation of the CDK inhibitor p27. Nat Cell Biol 1: 193–199.
12. Tsvetkov LM, Yeh KH, Lee SJ, Sun H, Zhang H, et al. (1999) p27(Kip1) ubiquitination and degradation is regulated by the SCF(Skp2) complex through phosphorylated Thr187 in p27. Curr Biol 9: 661–664.
13. Nakayama K, Nagahama H, Minamishima YA, Matsumoto M, Nakamichi I, et al. (2000) Targeted disruption of Skp2 results in accumulation of cyclin E and p27^{Kip1}, polyploidy and centrosome overdupication. EMBO J 19(9): 2069–2081.
14. Ganoth D, Bornstein G, Ko TK, Larsen B, Tyers M, et al. (2001) The cell-cycle regulatory protein Cks1 is required for SCF-Skp2-mediated ubiquitinylation of p27. Nat Cell Biol 3: 321–324.
15. Frescas D, Pagano M (2008) Deregulated proteolysis by the F-box proteins SKP2 and β-TrCP: tipping the scales of cancer. Nat Rev Cancer 8: 438–449.
16. Walton G, Buttyan R, Garcia ME, Olsson CA, Heusle TW, et al. (1992) Renal growth factor expression during the early phase of experimental hydronephrosis. J Urol 148: 510–514.
17. Saulo K, Jeremiah M (2002) Obstructive nephropathy and renal fibrosis. Am J Physiol Renal Physiol 283: F861–F875.
18. Gobe GC, Axelsen RA (1987) Genesis of renal tubular atrophy in experimental hydronephrosis in the rat. Role of apoptosis. Lab Invest 56: 273–281.

19. Morrissey JJ, Ishidoya S, McCracken R, Klahr S (1996) Control of p53 and p21 (WAF1) expression during unilateral ureteral obstruction. Kidney Int Suppl 57: S84–S92.
20. Gerth JH, Kriegsmann J, Trinh TT, Stahl RA, Wendt T, et al. (2002) Induction of p27^{Kip1} after unilateral ureteral obstruction is independent of angiotensis II. Kidney Int 61: 68–79.
21. Schaefer L, Macakova K, Raslik I, Micegova M, Gröne HJ, et al. (2002) Absence of decorin adversely influences tubulointerstitial fibrosis of the obstructed kidney by enhanced apoptosis and increased inflammatory reaction. Am J Pathol 160(3): 1181–1191.
22. Ophascharoensuk V, Fero ML, Hughes J, Roberts JM, Shankland SJ (1998) The cyclin-dependent kinases inhibitor p27^{kip1} safeguards against inflammatory injury. Nature Med 4: 575–58.
23. Hughes J, Brown P, Shankland SJ (1999) Cyclin kinase inhibitor p21$^{CIP1/WAF1}$ limits interstitial cell proliferation following ureteric obstruction. Am J Physiol 277: 948–956.
24. Suzuki S, Fukasawa H, Kitagawa K, Uchida C, Hattori T, et al. (2007) Renal damage in obstructive nephropathy is decreased in Skp2-deficient mice. Am J Pathol 171(2): 473–483.
25. Suzuki S, Fukasawa H, Misaki T, Togawa A, Ohashi N, et al. (2011) Up-regulation of Cks1 and Skp2 with TNFα/NF-κB signaling in chronic progressive nephropathy. Genes Cells 16(11): 1110–1120.
26. Bornstein G, Bloom J, Sitry-Shevah D, Nakayama K, Pagano M, et al. (2003) Role of the SCF^{Skp2} ubiquitin ligase in the degradation of p21Cip1 in S phase. J Biol Chem 278(28): 25752–25757.
27. Kamura T, Hara T, Kotoshiba S, Yada M, Ishida N, et al. (2003) Degradation of p57Kip2 mediated by SCFSkp2-dependent ubiquitylation. Proc Natl Acad Sci 100(18): 10231–10216.
28. von der Lehr N, Johansson S, Wu S, Bahram F, Castell A, et al. (2003) The F-box protein Skp2 participates in c-Myc proteosomal degradation and acts as a cofactor for c-Myc-regulated transcription. Mol Cell 11(5): 1189–1200.
29. Tedesco D, Lukas J, Reed SI (2002) The pRb-related protein p130 is regulated by phosphorylation-dependent proteolysis via the protein-ubiquitin ligase SCF(Skp2). Genes Dev 16(22): 2946–2957.
30. Hiramatsu Y, Kitagawa K, Suzuki T, Uchida C, Hattori T, et al. (2006) Degradation of Tob1 mediated by SCFSkp2-dependent ubiquitination. Cancer Res 66(17): 8477–8483.
31. Starostina NG, Kipreos ET (2012) Multiple degradation pathways regulate versatile CIP/KIP CDK inhibitors. Trends Cell Biol 22(1): 33–41.
32. Sicari BM, Troxell R, Salim F, Tanwir M, Takane KK, et al. (2012) c-myc and skp2 coordinate p27 degradation, vascular smooth muscle proliferation, and neointima formation induced by the parathyroid hormone-related protein. Endocrinology 153(2): 861–872.
33. Carew RM, Wang B, Kantharidis P (2011) The rople of EMT in renal fibrosis: Cell Tissue Res 347(1): 103–116.
34. Hay ED, Zuk A (1995) Transformations between epithelium and mesenchyme: normal, pathological, and experimentally induced. Am J Kidney Dis 26: 678–690.
35. Kalluri R, Neilson EG (2003) Epithelial-mesenchymal transition and its implications for fibrosis. J Clin Invest 112: 1776–1784.
36. Zeisberg M, Kalluri R (2004) The role epithelial-to mesenchymal transition in renal fibrosis. J Mol Med 82(3): 175–181.
37. Nakayama K, Ishida N, Shirane M, Inomata A, Inoue T, et al. (1996) Mice lacking p27(Kip1) display increased body size, multiple organ hyperplasia, retinal dysplasia, and pituitary tumors: Cell 85(5): 707–720.

Current Medicinal Chemistry, 2012, *19*, 893-900

Protein Degradation by the Ubiquitin-Proteasome Pathway and Organ Fibrosis

H. Fukasawa*[,1], Y. Fujigaki[2], T. Yamamoto[3], A. Hishida[4] and M. Kitagawa[5]

[1]*Renal Division, Department of Internal Medicine, Iwata City Hospital, Iwata, Shizuoka, Japan*

[2]*First Department of Medicine and* [3]*Department of Biochemistry I, Hamamatsu University School of Medicine, Hamamatsu, Shizuoka, Japan*

[3]*Second Department of Medicine, Clinical Training Center, Numazu City Hospital, Numazu, Shizuoka, Japan*

[4]*Department of Nephrology, Yaizu City Hospital, Yaizu, Shizuoka, Japan*

Abstract: Abnormal and exaggerated deposition of extracellular matrix proteins is the common feature of fibrotic diseases. The resulting fibrosis disrupts the normal architecture of the affected organs and finally leads to their dysfunction and failure. At present, there are no effective therapies for fibrotic diseases. Protein degradation *via* the ubiquitin-proteasome system is the major pathway for non-lysosomal proteolysis and controls many critical cellular functions including cell-cycle progression, deoxyribonucleic acid repair, growth and differentiation. Therefore, aberration of the system leads to dysregulation of cellular homeostasis and development of many diseases such as cancers, degenerative diseases and fibrotic diseases. Although the ubiquitin-proteasome system has mainly been investigated in the field of cancers so far and several anti-cancer drugs that modulate the activity of the system have been used clinically, the recent findings regarding the system and fibrosis can provide a rational basis for the discovery of novel therapy for fibrotic diseases. In this article, we discuss (i) the basic mechanism of the ubiquitin-proteasome system and (ii) the recent findings regarding the association between the system and pathological organ fibrosis. These examples indicate that the ubiquitin-proteasome system plays diverse roles in the progression of fibrotic diseases, and further studies of the system are expected to reveal new strategies for overcoming pathological fibrosis.

Keywords: E3 ubiquitin ligase, extracellular matrix, organ fibrosis, protein degradation, 26S proteasome and ubiquitin.

INTRODUCTION

All intracellular proteins and many extracellular proteins are persistently being degraded to their constituent amino acids and replaced by newly synthesized proteins. In humans, the amount of proteins turned over each day is quite large (3.5 - 4.5 g protein / kg / day). For example, approximately 280 g of protein is synthesized and degraded every day in a normal 70 kg adult, and the majority of these proteins are intracellular [1]. Accordingly, the overall rates of protein synthesis and degradation in the body must be balanced, because even a small decrease in synthesis or a small acceleration of degradation, if sustained, will result in a marked loss of protein stores (for example, malnutrition in cachexic patients with cancers) [1, 2]. Furthermore, the cellular proteolytic machinery must be highly selective and tightly regulated, because the accelerated destruction of an essential protein or the failure to degrade a short-lived regulatory protein could drastically alter cell function.

In this review, we discuss protein degradation *via* the ubiquitin-proteasome system (UPS), which is the pathway for the specific and selective proteolysis of intracellular proteins [3] and its relationship to the pathogenesis of organ fibrosis.

MAJOR PATHWAYS FOR PROTEIN DEGRADATION

Proteins are mainly degraded *via* two pathways in the body. These are the lysosomal degradation pathway and the UPS [4].

In the 1960s, Farquhar and Palade identified the functional significance of the lysosome [5, 6]. The lysosome mainly degrades extracellular proteins, such as the low-density lipoprotein (LDL) core particle, and peptide hormones, such as insulin. Before the degradation of the proteins by nonspecific lysosomal proteases, the proteins are internalized into the cell and routed to the lysosome by a series of intracellular vesicles. Lysosomal degradation accounts for approximately 20% of normal protein turnover. In addition, the lysosome also degrades cell surface membrane proteins, such as the LDL receptor. These proteins are targeted to the lysosome as membrane protein components in the same vesicles that route soluble internalized proteins [3].

The non-specificity of lysosomal proteases is the most characteristic feature of this system; all proteins exposed to the lysosome are generally degraded at the same rate. However, intracellular proteins have half-lives that vary from a few minutes to many days. In addition, specific inhibitors of lysosomal proteases have little effect on the degradation of intracellular proteins. These findings indicate that the lysosome is not the organelle that is responsible for specific and time-regulated intracellular proteolysis [3, 7]. The main function of intracellular proteolysis is to maintain the cell's quality control by removing misfolded, mutated, or damaged proteins. Through the removal of key regulatory proteins, such as enzymes and cell cycle regulators, intracellular proteolysis also controls basic cellular processes including metabolic pathways, cell cycle, and transcription. Therefore, it must be extremely specific and selective. To attain this high degree of specificity, the process consumes rather than produces metabolic energy [7].

PROTEIN DEGRADATION *VIA* THE UBIQUITIN-PROTEASOME SYSTEM

Degradation of proteins by the UPS is a tightly regulated and highly specific process that mainly degrades intracellular proteins [3]. Degradation of a target substrate by the UPS consists of two successive steps. The first step involves the conjugation of at least four or five ubiquitins to the targeted protein (called "poly-ubiquitination" or simply "ubiquitination"), a process that is catalyzed by the following three enzymes that act in concert: E1 (ubiquitin-activating enzyme), E2 (ubiquitin-conjugating enzyme) and E3 (ubiquitin ligase) (Fig. **1A**). E1 initiates ubiquitin ligation. Ubiquitin molecule is transferred from E1 to E2, which transiently carries ubiquitin moieties. E2 works in conjugation with E3, which is responsible for conferring substrate specificity. E3 mediates the transfer of ubiquitin to an internal lysine of the targeted protein and thereby poly-ubiquitin chain is conjugated to the target protein [3]. The second step is degradation of the ubiquitin-tagged substrate by the 26S proteasome complex, which recognizes lysine 48- or 11-linked poly-ubiquitin conjugated proteins (Fig. **1B**). The 26S proteasome is found in the nucleus and the cytosol of all cells and is composed of a central barrel-shaped 20S proteasome with a 19S

*Address correspondence to this author at the Renal Division, Department of Internal Medicine, Iwata City Hospital, 512-3 Ohkubo, Iwata, Shizuoka, 438-8550 Japan; Tel: +81-538-38-5000; Fax: +81-538-38-5050; E-mail: hfukasawaucsd@gmail.com

0929-8673/12 $58.00+.00

particle at either or both of its ends. After an ubiquitin-conjugated protein binds to the 19S particle, the poly-ubiquitin chain is cleaved off from the protein and disassembled so that the ubiquitins can be reused for the degradation of other proteins. Next, the protein cleaved off the poly-ubiquitin chain is unfolded in the base of the 19S particle. Linearization of the folded protein is essential to be translocated into the 20S particle, because the pore size of the particle is too narrow for globular proteins to enter [8]. After the substrate enters into the 20S's chamber, the polypeptide is cleaved to the small peptides that range from 3 to 15 residues in length. The derived small peptides are further degraded into individual amino acids by downstream cytosolic proteases to synthesize new proteins [9].

In the UPS, poly-ubiquitin conjugation to each targeted protein called poly-ubiquitination is a critical step in specific protein degradation, and the E3 enzyme is the key player in the selective recognition of each targeted protein [7].

FIBROSIS AS A COMMON PATHWAY OF ORGAN FAILURE

The fibrotic diseases include a wide spectrum of clinical entities such as scleroderma [10], the recently recognized nephrogenic systemic fibrosis [11, 12], which both diseases lead skin fibrosis, and organ-specific fibrosis of kidney [13, 14], heart [15], liver [16], bone marrow [17] and lung [18]. Although their etiologies and causative mechanisms are different, the fibrotic diseases share the common feature of abnormal and exaggerated deposition of extracellular matrix proteins in affected tissues. The persistent activation of fibroblastic cells distinguishes controlled repair occurring during normal wound healing from the uncontrolled fibrosis that is the hallmark of these diseases [19]. The resulting fibrosis disrupts the normal architecture of the affected organs and eventually leads to their dysfunction and failure. The progressive nature and the lack of effective treatment make these diseases more serious.

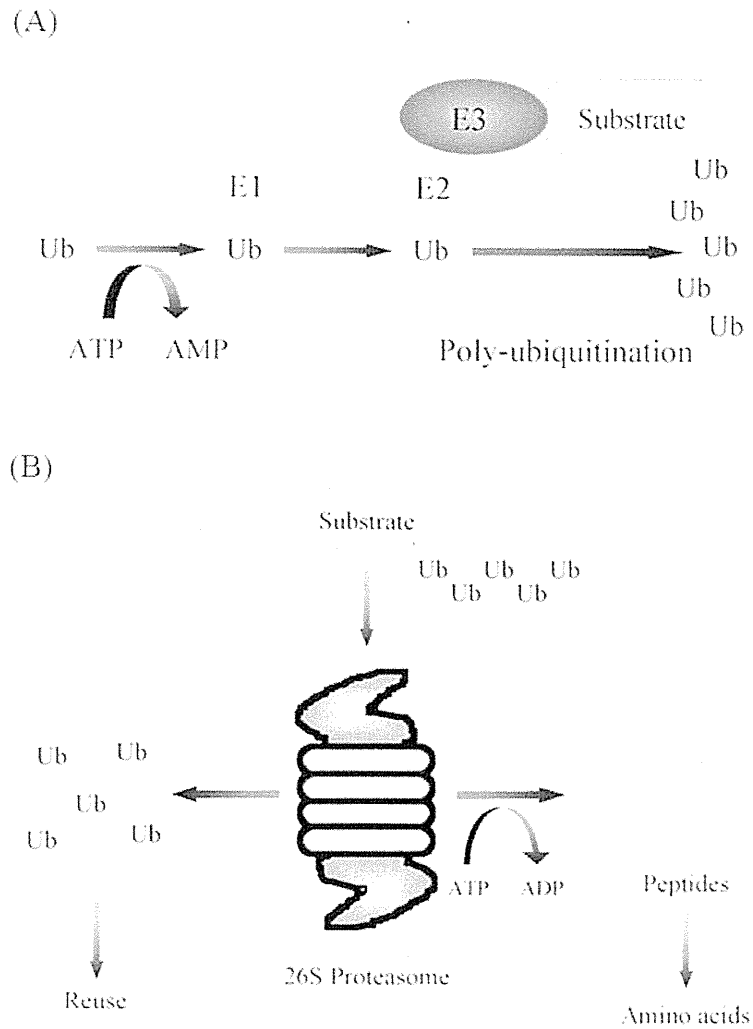

Fig. (1). Ubiquitin-Proteasome Pathway.

Degradation of a target substrate by the UPS involves two successive steps. (**A**) In the first step, ubiquitin (Ub) is activated and attached to an E1 (ubiquitin-activating enzyme) through a thioester bond. The ubiquitin is then transferred to an E2 (ubiquitin-conjugating enzyme), which functions together with an E3 (ubiquitin ligase). E3 mediates the transfer of ubiquitin to an internal lysine of the targeted substrate (Substrate) and thereby poly-ubiquitin chain is conjugated to the substrate (poly-ubiquitination), which serves as a protein degradation signal. (**B**) The second step is degradation of the ubiquitin-tagged substrate by the 26S proteasome complex. The 26S proteasome recognizes lysine 48- or 11-linked poly-ubiquitin conjugated proteins and degrades them to small peptides (3-15 amino acid residues). The derived peptides are further degraded into individual amino acids by cytosolic proteases. Detached ubiquitins are reusable.

Although the UPS has mainly been investigated in the field of cancers [20-22], neurodegenerative disorders such as autosomal recessive juvenile parkinsonism [23], Liddle syndrome [24], Fanconi anemia [25] and muscle wasting [1] so far, the recent findings regarding the UPS in the development of fibrotic diseases can provide a rational basis for the discovery of novel therapy for the diseases. Next, we discuss the relationship between the UPS and organ fibrosis.

EFFECTS OF PROTEASOMAL INHIBITION ON ORGAN FIBROSIS

As described in the previous sections, the UPS plays important roles in diverse cellular processes, and aberration of the system leads to dysregulation of cellular homeostasis and development of serious diseases. Therefore, it is not surprising that drugs such as proteasome inhibitors that modulate the activity of the UPS have the potential to treat various diseases including fibrosis.

Proteasome inhibitors are broadly categorized into two groups, synthetic analogues such as MG-132 (*N*-carbobenzoxy-Leu-Leu-leucinal), PSI (*N*-carbobenzoxy-L-gamma-t-butyl-L-glutamyl-L-alanyl-L-leucinal) and bortezomib (also known as Vercade® or PS-341), and natural products such as lactacystin (a metabolite of *Streptomyces lactacystinaeus*) and epoxomicin (a member of linear peptide epoxyketones) [26]. These inhibitors bind to the N-terminal of threonine residue of β subunit within the 20S proteasomes and inhibit those proteolytic activities. Although bortezomib, lactacystin and epoxomicin specifically inhibit proteasomes, MG-132 and PSI inhibit not only proteasomes but also cysteine proteases such as calpains and lysosomal cathepsins [9]. In particular, bortezomib has been reported to induce DNA damage, arrest cellular cycling at the G1/S or G2/M phase and suppress nuclear factor-κB (NF-κB) activity, and has widely been used for the treatment of multiple myeloma [20, 27-29].

To date, the effects of proteasome inhibitors on organ fibrosis have mainly been examined in animal models (Table 1). The earliest study on the therapeutic effect of proteasome inhibitors was in a rat model of obstructed nephropathy by unilateral ureteral obstruction (UUO), which is a model of tubulointerstitial fibrosis of kidneys. Administration of PSI inhibited the proteasomal activity and attenuated the enhanced expression of profibrotic proteins and development of tubulointerstitial fibrosis, which is a common pathway of progressive kidney diseases [30]. Another study examined the effect of MG-132 in spontaneously hypertensive rats. Systemic treatment with MG132 over 12 weeks effectively suppressed the myocardial expression of type I collagen mRNA and resulted in the attenuation of cardiac fibrosis, which is a cause of heart failure [31]. More recently, Hedhli *et al.* [32] reported that epoxomicin reversed cardiac hypertrophy and improved cardiac remodeling by aortic banding in a mouse model. Mice given epoxomicin from 2 weeks after aortic banding showed the suppression of increased NF-κB activity, collagen expressions and proteasomal activity. Other investigators examined the efficacy of proteasomal inhibition in liver fibrosis [33, 34]. First, Anan *et al.* [33] reported that the administration of bortezomib significantly attenuated α-smooth muscle actin and collagen expressions, as well as the severity of histological fibrosis in a mouse model of liver cirrhosis by bile duct ligation. Second, Pan *et al.* [34] reported that lactacystin prevented liver fibrosis in another mouse model of liver cirrhosis by administration of carbon tetrachloride. Bortezomib was also examined in a mouse model of bone marrow fibrosis by thrombopoietin over-expression. After 4 weeks of treatment, bortezomib decreased transforming growth factor (TGF) -β1 levels in bone marrow fluids and attenuated fibrosis of both bone marrow and spleen. After long-term treatment for 12 weeks, bortezomib attenuated osteosclerosis development and finally improved 1-year survival [35].

On the other hands, Fineschi *et al.* [36] reported that bortezomib failed to prevent lung fibrosis by bleomycin instillation in a mouse model and also failed to attenuate skin fibrosis in TSK-1/+ mice, which develop skin fibrosis in the absence of overt inflammation.

The mechanism of the effects of proteasome inhibitors on fibrotic diseases remains to be identified. One possible explanation is the inhibition of IκB (inhibitor of κB) degradation by the UPS and thereby suppresses NF-κB activation [37]. In fact, several investigators have reported that proteasome inhibitors attenuated organ fibrosis as well as suppression of NF-κB activation [30, 32]. Another possibility is the induction of matrix metalloproteinases (MMPs), which cause the degradation of extracellular matrix proteins. Recently, Catalgol *et al.* [38] have reported that proteasomal inhibition with lactacystin increased the expression of MMP-1 *via* activator protein-1 (AP-1) activation in skin fibroblasts.

In summary, it is suggested that the effects of proteasome inhibitors on fibrotic diseases are limited, and further studies are needed to clarify the precise mechanism of their therapeutic potential.

DYSREGULATION OF TGF-β/SMADS SIGNALING *VIA* THE UPS

Members of the TGF-β superfamily are pleiotropic cytokines that regulate numerous cellular functions including proliferation, differentiation, apoptosis, epithelial-mesenchymal transition, and accumulation of extracellular matrix proteins. They also play important physiological roles in embryonic development and wound healing as well as in pathological conditions such as carcinogenesis and organ fibrosis [39, 40]. TGF-β signaling is transmitted predominantly through cell surface serine and threonine kinase receptors to intracellular mediators known as Smads. The inhibitory Smad7 represses TGF-β signaling by interacting with activated TGF-β receptors, and down-regulation of Smad7

Table 1. Effects of Proteasome Inhibitors on Organ Fibrosis in Animal Models

Organ	Agent	Effect	Animal model	Reference
Kidney	PSI	Yes	Mouse obstructed nephropathy	[30]
Heart	MG-132	Yes	Spontaneously hypertensive rat	[31]
	Epoxomicin	Yes	Mouse submitted to aortic banding	[32]
Liver	Bortezomib	Yes	Mouse ligated bile duct	[33]
	Lactacystin	Yes	Mouse received carbon tetrachloride	[34]
Bone marrow	Bortezomib	Yes	Mouse with high thrombopoietin	[35]
Lung	Bortezomib	No	Mouse received bleomycin	[36]
Skin	Bortezomib	No	TSK-1/+ mouse	[36]

Definition of the abbreviation: PSI, *N*-carbobenzoxy-L-gamma-t-butyl-L-glutamyl-L-alanyl-L-leucinal and MG-132, *N*-carbobenzoxy-Leu-Leu-leucinal.

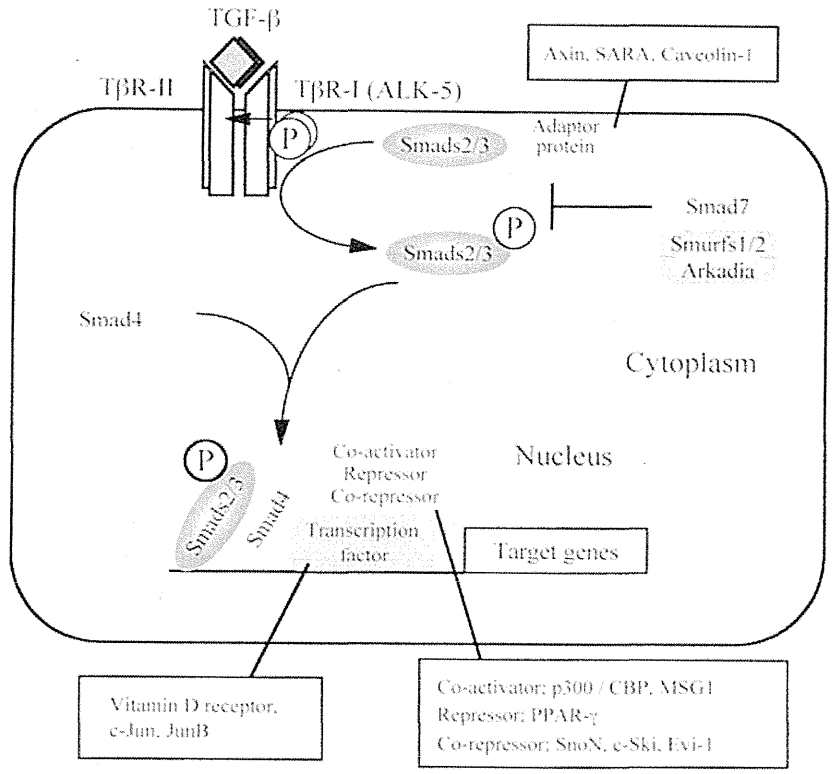

Fig. (2). TGF-β signaling *via* TGF-β receptors and Smads.

TGF-β signaling is transduced by transmembrane serine and threonine kinase receptors, termed TGF-β type I receptor (TβR-I) and TGF-β type II receptor (TβR-II), and intracellular mediators known as Smads. At first, activated TGF-β binds to TβR-II, which is intrinsically active. After the binding, the complex of TGF-β and TβR-II recruits TβR-I to phosphorylate it and then receptor-regulated Smads (Smad2 and Smad3) are phosphorylated (P) at serine residues in the carboxyl termini by the TβR-I (ALK-5; activin-like kinase-5). Once phosphorylated, Smads 2 and 3 dissociate from the receptor, bind to the common partner Smad (Smad4) and enter the nucleus. In the nucleus, activated Smads can interact with various transcriptional co-activators such as p300 or CBP, resulting in transcriptional activation. Alternatively, they form transcriptionally inactive complexes with repressors such as PPAR-γ, and co-repressors such as SnoN or c-Ski. Inhibitory Smad (Smad7) is an intracellular antagonist for TGF-β signaling that associates with activated TβR-I and hinders the activation of Smads 2 and 3 by preventing their interaction with activated TβR-I and consequent phosphorylation. List of abbreviations: ALK-5, activin-like kinase-5; CBP, CREB-binding protein; CREB, cAMP response element binding protein; Evi-1, ectopic viral integration site-1; MSG1, melanocyte-specific gene 1; PPAR-γ, peroxisome proliferator-activated receptor-γ; SARA, Smad anchor for receptor activation; Ski, Sloan-Kettering Institute proto-oncogene; Smurf, Smad-ubiquitination regulatory factor; and SnoN, *ski*-related novel gene N.

facilitates the effects of TGF-β *via* activation of Smads 2 and 3, which are the receptor-regulated Smads. After binding with the common partner Smad4, activated Smad complexes translocate into the nucleus to regulate target gene transcription in collaboration with specific transcriptional factors, co-activators, repressors and co-repressors [41, 42] (Fig. **2**).

TGF-β proteins are potent growth inhibitors in most cell types. Therefore, perturbations of TGF-β signaling are implicated in the progression of various cancers, as well as in development of inflammatory and fibrotic diseases [43]. For example, increased inhibitory Smad7 levels and decreased TGF-β activity are associated with enhanced inflammation in human inflammatory bowel disease [44]. In contrast, decreased Smad7 levels and increased TGF-β activity were observed in fibrotic tissues in scleroderma (skin) [45], myocardial infarction (heart) [46], and renal fibrosis (kidney) [47]. In chronic liver injury, the constitutive phosphorylation of Smad2 in the presence of low levels of endogenous Smad7 was implicated in the progression of liver fibrosis resulting in cirrhosis, whereas a transient increase in endogenous Smad7 inhibited the phosphorylation of Smad2 in acute and reversible liver injury [48]. These data suggest that profibrotic effects of TGF-β are critical in the progression of organ fibrosis, and cellular levels of Smads are important factors in the regulation of TGF-β signaling. On the other hand, Yang *et al.* [49] demonstrated that the levels of c-Ski (Sloan-Kettering Institute proto-oncogene) and SnoN (*ski*-related novel gene N) proteins, which are co-repressors of TGF-β, decreased progressively in renal fibrosis, and suggested that their decreased levels played a role in amplification of profibrotic TGF-β activity and resulted in the progression of renal fibrosis.

Several studies have demonstrated that TGF-β receptors, several Smads, c-Ski, and SnoN all undergo ubiquitin-proteasome mediated degradation [50-52]. Smad-ubiquitination regulatory factor 1 (Smurf1) was originally identified as a HECT (homologous to E6-AP C-terminus) type E3 ubiquitin ligase, which induces poly-ubiquitination and degradation of Smads 1 and 5 [53]. Smurf2, which is structurally similar to Smurf1, also targets Smad2 for degradation [54]. In addition, Smurfs 1 and 2 interact with nuclear Smad7 and induce the nuclear export of Smad7. The Smurfs / Smad7 complexes then associate with TGF-β type I receptor (TβR-I) and enhance its turnover [50, 51]. These findings suggest that Smurfs can negatively regulate TGF-β signaling by targeting their positive signaling components. In contrast to these findings, Bonni *et al.* [52] demonstrated that Smurf2 binds to transcriptional co-

repressor SnoN through activated Smad2, thereby targeting SnoN for ubiquitin-dependent degradation. Smurfs 1 and 2 have also been implicated in the ubiquitin-dependent degradation of inhibitory Smad7 during progression of renal fibrosis [47]. These findings could indicate that Smurf2 positively regulates TGF-β signaling under pathological conditions. Furthermore, Asano *et al.* [55] reported that the Smurf2-mediated inhibitory effect on TGF-β signaling was impaired in the fibroblasts of patients with scleroderma, whereas Smurf2 inhibited TGF-β signaling in normal human fibroblasts. Taken together, the role of Smurfs 1 and 2 in TGF-β signaling may change under pathological conditions such as fibrotic diseases. We also demonstrated that Smurf2 expression is rapidly induced by TGF-β itself [56]. Thus, the increased expression of Smurf2 by TGF-β in fibrotic tissues could be involved in the progression of diseases through protein degradation of Smad7 and SnoN, which are negative components of TGF-β signaling, resulting in further acceleration of TGF-β signaling followed by organ fibrosis. In accordance with these findings, it was shown that Smurf2 is mainly localized in tubular epithelial cells, that its level is increased in renal fibrosis [57] and that Smurf2 may be involved in the protein degradation of Smad7 and SnoN [47, 58, 59]. Therefore, Smurf2 can become one of therapeutic targets for fibrotic diseases, particularly renal fibrosis.

It is identified that Arkadia, a RING (really interesting new gene) finger-type E3 ubiquitin ligase, promotes ubiquitin-dependent degradation of Smad7 in collaboration with Axin, a scaffold protein [60, 61] (Fig. **2**). Liu *et al.* [62, 63] reported a close relationship between the reduction of Smad7 and the increase of Arkadia in a model of renal fibrosis and showed that Arkadia-Smad7-mediated positive regulation of TGF-β signaling can contribute to progression of the disease. Accordingly, Arkadia may also modulate organ fibrosis *via* enhanced TGF-β signaling caused by inhibitory Smad7 degradation.

METABOLIC DISEASES SUCH AS DIABETES AND THE UPS

Diabetic nephropathy is one of the major complications of diabetes mellitus and is the leading cause of end-stage kidney diseases. Diabetic nephropathy is characterized by increased urinary protein excretion, renal hypertrophy, thickening of the glomerular and tubular basement membranes, and mesangial matrix expansion with extracellular matrix protein deposition, which is followed by tubulointerstitial fibrosis [64]. High levels of glucose and various growth factors, such as TGF-β, were shown to contribute to the accumulation of extracellular matrix proteins in the affected tissues, resulting in fibrosis [65]. In a rat model of diabetic nephropathy induced by streptozotocin, it has been reported that MG-132 administration prevented increased 24-hr urinary protein excretion rate and pathological changes [66].

Insulin resistance associated with diabetes and obesity is a physiological condition where insulin becomes less effective at lowering blood sugar levels. The peroxisome proliferator-activated receptor-γ (PPAR-γ) is a ligand-activated nuclear receptor involved in a number of physiological processes including adipocyte differentiation, glucose metabolism, lipid homeostasis and monocyte / macrophage differentiation [67, 68]. PPAR-γ also influences fatty acid storage in adipose tissue and is implicated in insulin resistance and atherosclerosis [67, 68]. Synthetic PPAR-γ agonists, such as pioglitazone and rosiglitazone, are clinically used as insulin sensitizers to treat patients with type2 diabetes [69]. Furthermore, the beneficial effects of PPAR-γ agonists include the lowering of blood pressure, triglyceride reduction and elevation of high-density lipoprotein-cholesterol [70]. Recently, it has been reported that PPAR-γ is degraded *via* the UPS, although the responsible E3 ligase has not been identified [71, 72], and its agonists inhibit the development of liver, kidney and skin fibrosis [73-75]. Because PPAR-γ is known as a transcriptional repressor of TGF-β [76, 77] (Fig. **2**), the therapeutic potential of PPAR-γ agonists is supposed to be mediated by inhibition of TGF-β signaling, at least partially.

REGULATION OF $p27^{kip1}$ BY THE UPS IN CANCERS AND FIBROTIC DISEASES

$p27^{kip1}$ (p27) is a cell cycle inhibitor and a tumor suppressor [78, 79]. Various studies have shown a decrease in p27 protein in many cancers including gliomas, lymphomas and cancer of the colorectum, prostate, lung, head and neck [80-82]. However, it has been reported that the level of p27 mRNA remains constant or inversely increases in spite of decreased p27 protein [83-85]. The discrepancy between protein and mRNA levels in the cancers is consistent with evidence that the level of p27 protein is mainly regulated *via* protein degradation. The mechanism that underlies the low level of p27 protein in cancers involves an abnormally enhanced degradation by the UPS as a result of over-expression of S-phase kinase-associated protein 2 (Skp2), the E3 ubiquitin ligase of p27 [86]. Because Skp2 has oncogenic potential, it sensitizes to different tumors when over-expressed in mice [87]. In accordance with this finding, many researchers have demonstrated a correlation between low levels of p27, high levels of Skp2, tumor grading, clinical stage and overall prognosis in colorectal [88], breast [89], prostate [90], and other types of cancer [82].

In the progression of fibrotic diseases, the regulation of p27 levels is more complicated than in the progression of cancers. It has been reported that the levels of p27 protein are increased in obstructed nephropathy by UUO, a model of tubulointerstitial fibrosis of the kidneys [91]. Using p27 knockout mice, Ophascharoensuk *et al.* [92] showed that p27 plays renoprotective roles in the development of tubulointerstitial fibrosis of the kidneys. These observations indicate that increased levels of p27 protein serve as the compensatory response to protect the kidneys against fibrosis.

Recently, we reported that Skp2 is involved in the development of tubulointerstitial fibrosis of the kidneys by UUO. We showed that Skp2 mRNA expression is up-regulated in the model, the increased levels of p27 protein are significantly higher in Skp2 knockout mice than the levels in wild-type mice, and p27 accumulation is involved in the amelioration of tubulointerstitial fibrosis [93]. We also found that cdc kinase subunit 1 (Cks1), which is an essential cofactor for the Skp / Cullin / F-box (SCF)-Skp2 ubiquitin ligase in targeting p27, is up-regulated *via* tumor necrosis factor (TNF)-α/ NF-κB signaling in the same model [94]. These observations indicate that p27 protein levels are increased to protect the kidneys under fibrotic conditions, but that the absolute level may not be enough to prevent fibrosis. Thus, progressive renal damage is maintained, because protein degradation of p27 *via* Skp2 occurs simultaneously.

In summary, it is suggested that the balance between production and degradation is important in the case of p27 protein, and the absolute level of p27 protein is mainly regulated *via* protein degradation in both organ fibrosis and cancers. However, further studies are needed to better understand the relationship between p27 and Skp2 in the progression of fibrotic diseases.

CONCLUSIONS AND FUTURE PERSPECTIVES

The UPS is involved in TGF-β / Smads signaling pathway, metabolic diseases, regulation of p27 protein and undoubtedly the pathogenesis of organ fibrosis. Proteasome inhibitors are effective on the prevention of organ fibrosis in several animal models, at least partially, although there are no effective therapies for human fibrotic diseases to date.

At present, Vercade® (bortezomib or PS-341), a proteasome inhibitor, has been used as one option of the treatment for multiple myeloma. One possible therapeutic strategy for fibrotic diseases may be combined therapies of proteasome inhibitors with the drugs that affect the TGF-β pathway such as PPAR-γ agonists [76, 77] or monoclonal antibodies against TGF- β [95, 96]. However, the significant problem of proteasome inhibitors as a therapeutic strategy of chronic diseases including fibrosis is the low specificity for each substrate. Accordingly, new and highly specific drugs that target the degradation pathway of a single or a few proteins without affecting others are expected. Those novel drugs, which ideally affect E3 ligases, should have far fewer adverse effects than proteasome inhibitors, which is less specific. For example, specific inhibitors against SCF-Skp2/Cks1 E3 ligase, which protect p27 degradation, may be applicable for the treatment of renal fibrosis.

In the near future, new, potent and highly specific drugs that modulate the activity of the UPS may be available, although further studies are needed to discover new drugs for overcoming organ fibrosis.

ACKNOWLEDGMENTS

This work was supported by Grants-in-Aid for Scientific Research from Japan Society for the Promotion of Science (No. 17790549) and Japanese Association of Dialysis Physicians Grant from Japanese Association of Dialysis Physicians (JADP Grant 2011-08).

CONFLICTS OF INTEREST

None.

ABBREVIATIONS

ALK-5 = activin-like kinase-5
AMP = adenosine monophosphate
AP-1 = activator protein-1
ATP = adenosine triphosphate
CBP = CREB-binding protein
Cks1 = cdc kinase subunit 1
CREB = cAMP response element binding protein
DNA = deoxyribonucleic acid
Evi-1 = ectopic viral integration site-1
HECT = homologous to E6-AP C-terminus
IκB = inhibitor of κB
LDL = low-density lipoprotein
MG-132 = *N*-carbobenzoxy-Leu-Leu-leucinal
MMP = matrix metalloproteinase
MSG1 = melanocyte-specific gene 1
NF-κB = nuclear factor-κB
p27 = $p27^{kip1}$
PPAR-γ = peroxisome proliferator-activated receptor-γ
PSI = *N*-carbobenzoxy-L-gamma-t-butyl-L-glutamyl-L-alanyl-L-leucinal
RING = really interesting new gene
SARA = Smad anchor for receptor activation
SCF = Skp/Cullin/F-box
Ski = Sloan-Kettering Institute proto-oncogene
Skp2 = S-phase kinase-associated protein 2
Smurf1 = Smad-ubiquitination regulatory factor 1
SnoN = *ski*-related novel gene N
TGF = transforming growth factor
TNF = Tumor necrosis factor
TβR-I = TGF-β type I receptor
TβR-II = TGF-β type II receptor
UPS = ubiquitin-proteasome system
UUO = unilateral ureteral obstruction

REFERENCES

[1] Mitch, W.E.; Goldberg, A.L. Mechanisms of muscle wasting. The role of the ubiquitin-proteasome pathway. *N Engl J Med*, **1996**, *335*(25), 1897-1905.
[2] Rajan, V.; Mitch, W.E. Ubiquitin, proteasomes and proteolytic mechanisms activated by kidney disease. *Biochim Biophys Acta*, **2008**, *1782*(12), 795-799.
[3] Glickman, M.H.; Ciechanover, A. The ubiquitin-proteasome proteolytic pathway: destruction for the sake of construction. *Physiol Rev*, **2002**, *82*(2), 373-428.
[4] Knecht, E.; Aguado, C.; Carcel, J.; Esteban, I.; Esteve, J.M.; Ghislat, G.; Moruno, J.F.; Vidal, J.M.; Saez, R. Intracellular protein degradation in mammalian cells: recent developments. *Cell Mol Life Sci*, **2009**, *66*(15), 2427-2443.
[5] Farquhar, M.G.; Palade, G.E. FUNCTIONAL EVIDENCE FOR THE EXISTENCE OF A THIRD CELL TYPE IN THE RENAL GLOMERULUS : Phagocytosis of Filtration Residues by a Distinctive "Third" Cell. *J Cell Biol*, **1962**, *13*(1), 55-87.
[6] Smith, R.E.; Farquhar, M.G. Lysosome function in the regulation of the secretory process in cells of the anterior pituitary gland. *J Cell Biol*, **1966**, *31*(2), 319-347.
[7] Reinstein, E.; Ciechanover, A. Narrative review: protein degradation and human diseases: the ubiquitin connection. *Ann Intern Med*, **2006**, *145*(9), 676-684.
[8] Groll, M.; Bajorek, M.; Kohler, A.; Moroder, L.; Rubin, D.M.; Huber, R.; Glickman, M.H.; Finley, D. A gated channel into the proteasome core particle. *Nat Struct Biol*, **2000**, 7(11), 1062-1067.
[9] Tanaka, K. The proteasome: overview of structure and functions. *Proc Jpn Acad Ser B Phys Biol Sci*, **2009**, *85*(1), 12-36.
[10] Varga, J.; Abraham, D. Systemic sclerosis: a prototypic multisystem fibrotic disorder. *J Clin Invest*, **2007**, *117*(3), 557-567.
[11] Mendoza, F.A.; Artlett, C.M.; Sandorfi, N.; Latinis, K.; Piera-Velazquez, S.; Jimenez, S.A. Description of 12 cases of nephrogenic fibrosing dermopathy and review of the literature. *Semin Arthritis Rheum*, **2006**, *35*(4), 238-249.
[12] Cowper, S.E. Nephrogenic systemic fibrosis: an overview. *J Am Coll Radiol*, **2008**, *5*(1), 23-28.
[13] Schnaper, H.W. Renal fibrosis. *Methods Mol Med*, **2005**, *117*, 45-68.
[14] Venkatachalam, M.A.; Griffin, K.A.; Lan, R.; Geng, H.; Saikumar, P.; Bidani, A.K. Acute kidney injury: a springboard for progression in chronic kidney disease. *Am J Physiol Renal Physiol*.
[15] Lijnen, P.J.; Petrov, V.V.; Fagard, R.H. Induction of cardiac fibrosis by angiotensin II. *Methods Find Exp Clin Pharmacol*, **2000**, *22*(10), 709-723.
[16] Tsukada, S.; Parsons, C.J.; Rippe, R.A. Mechanisms of liver fibrosis. *Clin Chim Acta*, **2006**, *364*(1-2), 33-60.
[17] Thiele, J.; Kvasnicka, H.M.; Zankovich, R.; Diehl, V. Clinical and morphological criteria for the diagnosis of prefibrotic idiopathic (primary) myelofibrosis. *Ann Hematol*, **2001**, *80*(3), 160-165.
[18] Gross, T.J.; Hunninghake, G.W. Idiopathic pulmonary fibrosis. *N Engl J Med*, **2001**, *345*(7), 517-525.
[19] Jimenez, S.A.; Hitraya, E.; Varga, J. Pathogenesis of scleroderma. Collagen. *Rheum Dis Clin North Am*, **1996**, *22*(4), 647-674.
[20] Richardson, P.G.; Barlogie, B.; Berenson, J.; Singhal, S.; Jagannath, S.; Irwin, D.; Rajkumar, S.V.; Srkalovic, G.; Alsina, M.; Alexanian, R.; Siegel, D.; Orlowski, R.Z.; Kuter, D.; Limentani, S.A.; Lee, S.; Hideshima, T.; Esseltine, D.L.; Kauffman, M.; Adams, J.; Schenkein, D.P.; Anderson, K.C. A phase 2 study of bortezomib in relapsed, refractory myeloma. *N Engl J Med*, **2003**, *348*(26), 2609-2617.
[21] Boccadoro, M.; Morgan, G.; Cavenagh, J. Preclinical evaluation of the proteasome inhibitor bortezomib in cancer therapy. *Cancer Cell Int*, **2005**, *5*(1), 18.
[22] Ludwig, H.; Khayat, D.; Giaccone, G.; Facon, T. Proteasome inhibition and its clinical prospects in the treatment of hematologic and solid malignancies. *Cancer*, **2005**, *104*(9), 1794-1807.
[23] Kitada, T.; Asakawa, S.; Hattori, N.; Matsumine, H.; Yamamura, Y.; Minoshima, S.; Yokochi, M.; Mizuno, Y.; Shimizu, N. Mutations in the parkin gene cause autosomal recessive juvenile parkinsonism. *Nature*, **1998**, *392*(6676), 605-608.
[24] Staub, O.; Gautschi, I.; Ishikawa, T.; Breitschopf, K.; Ciechanover, A.;

Schild, L.; Rotin, D. Regulation of stability and function of the epithelial Na+ channel (ENaC) by ubiquitination. *EMBO J.* **1997**, *16*(21), 6325-6336.

[25] Jacquemont, C.; Taniguchi, T. The Fanconi anemia pathway and ubiquitin. *BMC Biochem.* **2007**, *8 Suppl 1*, S10.

[26] Myung, J.; Kim, K.B.; Crews, C.M. The ubiquitin-proteasome pathway and proteasome inhibitors. *Med Res Rev.* **2001**, *21*(4), 245-273.

[27] Adams, J.; Palombella, V.J.; Sausville, E.A.; Johnson, J.; Destree, A.; Lazarus, D.D.; Maas, J.; Pien, C.S.; Prakash, S.; Elliott, P.J. Proteasome inhibitors: a novel class of potent and effective antitumor agents. *Cancer Res.* **1999**, *59*(11), 2615-2622.

[28] Sunwoo, J.B.; Chen, Z.; Dong, G.; Yeh, N.; Crowl Bancroft, C.; Sausville, E.; Adams, J.; Elliott, P.; Van Waes, C. Novel proteasome inhibitor PS-341 inhibits activation of nuclear factor-kappa B, cell survival, tumor growth, and angiogenesis in squamous cell carcinoma. *Clin Cancer Res.* **2001**, *7*(5), 1419-1428.

[29] An, J.; Sun, Y.; Fisher, M.; Rettig, M.B. Maximal apoptosis of renal cell carcinoma by the proteasome inhibitor bortezomib is nuclear factor-kappaB dependent. *Mol Cancer Ther.* **2004**, *3*(6), 727-736.

[30] Tashiro, K.; Tamada, S.; Kuwabara, N.; Komiya, T.; Takekida, K.; Asai, T.; Iwao, H.; Sugimura, K.; Matsumura, Y.; Takaoka, M.; Nakatani, T.; Miura, K. Attenuation of renal fibrosis by proteasome inhibition in rat obstructive nephropathy: possible role of nuclear factor kappaB. *Int J Mol Med.* **2003**, *12*(4), 587-592.

[31] Meiners, S.; Hocher, B.; Weller, A.; Laule, M.; Stangl, V.; Guenther, C.; Godes, M.; Mrozikiewicz, A.; Baumann, G.; Stangl, K. Downregulation of matrix metalloproteinases and collagens and suppression of cardiac fibrosis by inhibition of the proteasome. *Hypertension.* **2004**, *44*(4), 471-477.

[32] Hedhli, N.; Lizano, P.; Hong, C.; Fritzky, L.F.; Dhar, S.K.; Liu, H.; Tian, Y.; Gao, S.; Madura, K.; Vatner, S.F.; Depre, C. Proteasome inhibition decreases cardiac remodeling after initiation of pressure overload. *Am J Physiol Heart Circ Physiol.* **2008**, *295*(4), H1385-1393.

[33] Anan, A.; Baskin-Bey, E.S.; Isomoto, H.; Mott, J.L.; Bronk, S.F.; Albrecht, J.H.; Gores, G.J. Proteasome inhibition attenuates hepatic injury in the bile duct-ligated mouse. *Am J Physiol Gastrointest Liver Physiol.* **2006**, *291*(4), G709-716.

[34] Pan, X.; Hussain, F.N.; Iqbal, J.; Feuerman, M.H.; Hussain, M.M. Inhibiting proteasomal degradation of microsomal triglyceride transfer protein prevents CCl4-induced steatosis. *J Biol Chem.* **2007**, *282*(23), 17078-17089.

[35] Wagner-Ballon, O.; Pisani, D.F.; Gastinne, T.; Tulliez, M.; Chaligne, R.; Lacout, C.; Aurade, F.; Villeval, J.L.; Gonin, P.; Vainchenker, W.; Giraudier, S. Proteasome inhibitor bortezomib impairs both myelofibrosis and osteosclerosis induced by high thrombopoietin levels in mice. *Blood.* **2007**, *110*(1), 345-353.

[36] Fineschi, S.; Bongiovanni, M.; Donati, Y.; Djaafar, S.; Naso, F.; Goffin, L.; Argiroffo, C.B.; Pache, J.C.; Dayer, J.M.; Ferrari-Lacraz, S.; Chizzolini, C. *In vivo* investigations on anti-fibrotic potential of proteasome inhibition in lung and skin fibrosis. *Am J Respir Cell Mol Biol.* **2008**, *39*(4), 458-465.

[37] Guijarro, C.; Egido, J. Transcription factor-kappa B (NF-kappa B) and renal disease. *Kidney Int.* **2001**, *59*(2), 415-424.

[38] Catalgol, B.; Ziaja, I.; Breusing, N.; Jung, T.; Hohn, A.; Alpertunga, B.; Schroeder, P.; Chondrogianni, N.; Gonos, E.S.; Petropoulos, I.; Friguet, B.; Klotz, L.O.; Krutmann, J.; Grune, T. The proteasome is an integral part of solar ultraviolet a radiation-induced gene expression. *J Biol Chem.* **2009**, *284*(44), 30076-30086.

[39] Massague, J. TGF-beta signal transduction. *Annu Rev Biochem.* **1998**, *67*, 753-791.

[40] Border, W.A.; Ruoslahti, E. Transforming growth factor-beta in disease: the dark side of tissue repair. *J Clin Invest.* **1992**, *90*(1), 1-7.

[41] Izzi, L.; Attisano, L. Regulation of the TGFbeta signalling pathway by ubiquitin-mediated degradation. *Oncogene.* **2004**, *23*(11), 2071-2078.

[42] Fukasawa, H.; Yamamoto, T.; Kitagawa, K.; Hishida, A. Regulation of TGF-beta signaling by Smads and its roles in tissue fibrosis. *Current Signal Transduction Therapy.* **2008**, *3*(1), 1-6.

[43] Fukasawa, H.; Yamamoto, T.; Fujigaki, Y.; Misaki, T.; Ohashi, N.; Takayama, T.; Suzuki, S.; Mugiya, S.; Oda, T.; Uchida, C.; Kitagawa, K.; Hattori, T.; Hayashi, H.; Ozono, S.; Kitagawa, M.; Hishida, A. Reduction of transforming growth factor-beta type II receptor is caused by the enhanced ubiquitin-dependent degradation in human renal cell carcinoma. *Int J Cancer.* **2011**, *127*(7), 1517-1525.

[44] Monteleone, G.; Kumberova, A.; Croft, N.M.; McKenzie, C.; Steer, H.W.; MacDonald, T.T. Blocking Smad7 restores TGF-beta1 signaling in chronic inflammatory bowel disease. *J Clin Invest.* **2001**, *108*(4), 601-609.

[45] Dong, C.; Zhu, S.; Wang, T.; Yoon, W.; Li, Z.; Alvarez, R.J.; ten Dijke, P.; White, B.; Wigley, F.M.; Goldschmidt-Clermont, P.J. Deficient Smad7 expression: a putative molecular defect in scleroderma. *Proc Natl Acad Sci U S A.* **2002**, *99*(6), 3908-3913.

[46] Wang, B.; Hao, J.; Jones, S.C.; Yee, M.S.; Roth, J.C.; Dixon, I.M. Decreased Smad 7 expression contributes to cardiac fibrosis in the infarcted rat heart. *Am J Physiol Heart Circ Physiol.* **2002**, *282*(5), H1685-1696.

[47] Fukasawa, H.; Yamamoto, T.; Togawa, A.; Ohashi, N.; Fujigaki, Y.; Oda, T.; Uchida, C.; Kitagawa, K.; Hattori, T.; Suzuki, S.; Kitagawa, M.; Hishida, A. Down-regulation of Smad7 expression by ubiquitin-dependent degradation contributes to renal fibrosis in obstructive nephropathy in mice. *Proc Natl Acad Sci U S A.* **2004**, *101*(23), 8687-8692.

[48] Tahashi, Y.; Matsuzaki, K.; Date, M.; Yoshida, K.; Furukawa, F.; Sugano, Y.; Matsushita, M.; Himeno, Y.; Inagaki, Y.; Inoue, K. Differential regulation of TGF-beta signal in hepatic stellate cells between acute and chronic rat liver injury. *Hepatology.* **2002**, *35*(1), 49-61.

[49] Yang, J.; Zhang, X.; Li, Y.; Liu, Y. Downregulation of Smad transcriptional corepressors SnoN and Ski in the fibrotic kidney: an amplification mechanism for TGF-beta1 signaling. *J Am Soc Nephrol.* **2003**, *14*(12), 3167-3177.

[50] Kavsak, P.; Rasmussen, R.K.; Causing, C.G.; Bonni, S.; Zhu, H.; Thomsen, G.H.; Wrana, J.L. Smad7 binds to Smurf2 to form an E3 ubiquitin ligase that targets the TGF beta receptor for degradation. *Mol Cell.* **2000**, *6*(6), 1365-1375.

[51] Ebisawa, T.; Fukuchi, M.; Murakami, G.; Chiba, T.; Tanaka, K.; Imamura, T.; Miyazono, K. Smurf1 interacts with transforming growth factor-beta type I receptor through Smad7 and induces receptor degradation. *J Biol Chem.* **2001**, *276*(16), 12477-12480.

[52] Bonni, S.; Wang, H.R.; Causing, C.G.; Kavsak, P.; Stroschein, S.L.; Luo, K.; Wrana, J.L. TGF-beta induces assembly of a Smad2-Smurf2 ubiquitin ligase complex that targets SnoN for degradation. *Nat Cell Biol.* **2001**, *3*(6), 587-595.

[53] Zhu, H.; Kavsak, P.; Abdollah, S.; Wrana, J.L.; Thomsen, G.H. A SMAD ubiquitin ligase targets the BMP pathway and affects embryonic pattern formation. *Nature.* **1999**, *400*(6745), 687-693.

[54] Lin, X.; Liang, M.; Feng, X.H. Smurf2 is a ubiquitin E3 ligase mediating proteasome-dependent degradation of Smad2 in transforming growth factor-beta signaling. *J Biol Chem.* **2000**, *275*(47), 36818-36822.

[55] Asano, Y.; Ihn, H.; Yamane, K.; Kubo, M.; Tamaki, K. Impaired Smad7-Smurf-mediated negative regulation of TGF-beta signaling in scleroderma fibroblasts. *J Clin Invest.* **2004**, *113*(2), 253-264.

[56] Ohashi, N.; Yamamoto, T.; Uchida, C.; Togawa, A.; Fukasawa, H.; Fujigaki, Y.; Suzuki, S.; Kitagawa, K.; Hattori, T.; Oda, T.; Hayashi, H.; Hishida, A.; Kitagawa, M. Transcriptional induction of Smurf2 ubiquitin ligase by TGF-beta. *FEBS Lett.* **2005**, *579*(12), 2557-2563.

[57] Tan, R.; He, W.; Lin, X.; Kiss, L.P.; Liu, Y. Smad ubiquitination regulatory factor-2 in the fibrotic kidney: regulation, target specificity, and functional implication. *Am J Physiol Renal Physiol.* **2008**, *294*(5), F1076-1083.

[58] Togawa, A.; Yamamoto, T.; Suzuki, H.; Fukasawa, H.; Ohashi, N.; Fujigaki, Y.; Kitagawa, K.; Hattori, T.; Kitagawa, M.; Hishida, A. Ubiquitin-dependent degradation of Smad2 is increased in the glomeruli of rats with anti-thymocyte serum nephritis. *Am J Pathol.* **2003**, *163*(4), 1645-1652.

[59] Fukasawa, H.; Yamamoto, T.; Togawa, A.; Ohashi, N.; Fujigaki, Y.; Oda, T.; Uchida, C.; Kitagawa, K.; Hattori, T.; Suzuki, S.; Kitagawa, M.; Hishida, A. Ubiquitin-dependent degradation of SnoN and Ski is increased in renal fibrosis induced by obstructive injury. *Kidney Int.* **2006**, *69*(10), 1733-1740.

[60] Koinuma, D.; Shinozaki, M.; Komuro, A.; Goto, K.; Saitoh, M.; Hanyu, A.; Ebina, M.; Nukiwa, T.; Miyazawa, K.; Imamura, T.; Miyazono, K. Arkadia amplifies TGF-beta superfamily signalling through degradation of Smad7. *EMBO J.* **2003**, *22*(24), 6458-6470.

[61] Liu, W.; Rui, H.; Wang, J.; Lin, S.; He, Y.; Chen, M.; Li, Q.; Ye, Z.; Zhang, S.; Chan, S.C.; Chen, Y.G.; Han, J.; Lin, S.C. Axin is a scaffold protein in TGF-beta signaling that promotes degradation of Smad7 by Arkadia. *EMBO J.* **2006**, *25*(8), 1646-1658.

[62] Liu, F.Y.; Li, X.Z.; Peng, Y.M.; Liu, H.; Liu, Y.H. Arkadia-Smad7-mediated positive regulation of TGF-beta signaling in a rat model of tubulointerstitial fibrosis. *Am J Nephrol.* **2007**, *27*(2), 176-183.

[63] Liu, F.Y.; Li, X.Z.; Peng, Y.M.; Liu, H.; Liu, Y.H. Arkadia regulates TGF-beta signaling during renal tubular epithelial to mesenchymal cell transition. *Kidney Int.* **2008**, *73*(5), 588-594.

[64] Mauer, S.M.; Steffes, M.W.; Ellis, E.N.; Sutherland, D.E.; Brown, D.M.; Goetz, F.C. Structural-functional relationships in diabetic nephropathy. *J Clin Invest.* **1984**, *74*(4), 1143-1155.

[65] Sharma, K.; Ziyadeh, F.N. Hyperglycemia and diabetic kidney disease. The case for transforming growth factor-beta as a key mediator. *Diabetes.* **1995**, *44*(10), 1139-1146.

[66] Luo, Z.F.; Qi, W.; Feng, B.; Mu, J.; Zeng, W.; Guo, Y.H.; Pang, Q.; Ye, Z.L.; Liu, L.; Yuan, F.H. Prevention of diabetic nephropathy in rats through enhanced renal antioxidative capacity by inhibition of the proteasome. *Life Sci.* **88**(11-12), 512-520.

[67] Guan, Y.; Zhang, Y.; Breyer, M.D. The Role of PPARs in the Transcriptional Control of Cellular Processes. *Drug News Perspect.* **2002**, *15*(3), 147-154.

[68] Semple, R.K.; Chatterjee, V.K.; O'Rahilly, S. PPAR gamma and human metabolic disease. *J Clin Invest.* **2006**, *116*(3), 581-589.

[69] Czoski-Murray, C.; Warren, E.; Chilcott, J.; Beverley, C.; Psyllaki, M.A.; Cowan, J. Clinical effectiveness and cost-effectiveness of pioglitazone and rosiglitazone in the treatment of type 2 diabetes: a systematic review and economic evaluation. *Health Technol Assess.* **2004**, *8*(13), iii, ix-x, 1-91.

[70] Chiquette, E.; Ramirez, G.; Defronzo, R. A meta-analysis comparing the effect of thiazolidinediones on cardiovascular risk factors. *Arch Intern Med.* **2004**, *164*(19), 2097-2104.

[71] Hauser, S.; Adelmant, G.; Sarraf, P.; Wright, H.M.; Mueller, E.; Spiegelman, B.M. Degradation of the peroxisome proliferator-activated receptor gamma is linked to ligand-dependent activation. *J Biol Chem.* **2000**, *275*(24), 18527-18533.

[72] Blanquart, C.; Barbier, O.; Fruchart, J.C.; Staels, B.; Glineur, C. Peroxisome proliferator-activated receptor alpha (PPARalpha) turnover by the ubiquitin-

proteasome system controls the ligand-induced expression level of its target genes. *J Biol Chem*, **2002**, *277*(40), 37254-37259.

[73] Chen, H.; He, Y.W.; Liu, W.Q.; Zhang, J.H. Rosiglitazone prevents murine hepatic fibrosis induced by Schistosoma japonicum. *World J Gastroenterol*, **2008**, *14*(18), 2905-2911.

[74] Kawai, T.; Masaki, T.; Doi, S.; Arakawa, T.; Yokoyama, Y.; Doi, T.; Kohno, N.; Yorioka, N. PPAR-gamma agonist attenuates renal interstitial fibrosis and inflammation through reduction of TGF-beta. *Lab Invest*, **2009**, *89*(1), 47-58.

[75] Wu, M.; Melichian, D.S.; Chang, E.; Warner-Blankenship, M.; Ghosh, A.K.; Varga, J. Rosiglitazone abrogates bleomycin-induced scleroderma and blocks profibrotic responses through peroxisome proliferator-activated receptor-gamma. *Am J Pathol*, **2009**, *174*(2), 519-533.

[76] Weigert, C.; Brodbeck, K.; Bierhaus, A.; Haring, H.U.; Schleicher, E.D. c-Fos-driven transcriptional activation of transforming growth factor beta-1: inhibition of high glucose-induced promoter activity by thiazolidinediones. *Biochem Biophys Res Commun*, **2003**, *304*(2), 301-307.

[77] Lee, C.H.; Kim, H.D.; Shin, S.M.; Kim, S.G. A Novel Mechanism of PPARgamma Regulation of TGFbeta1: Implication in Cancer Biology. *PPAR Res*, **2008**, *2008*, 762398.

[78] Polyak, K.; Kato, J.Y.; Solomon, M.J.; Sherr, C.J.; Massague, J.; Roberts, J.M.; Koff, A. p27Kip1, a cyclin-Cdk inhibitor, links transforming growth factor-beta and contact inhibition to cell cycle arrest. *Genes Dev*, **1994**, *8*(1), 9-22.

[79] Polyak, K.; Lee, M.H.; Erdjument-Bromage, H.; Koff, A.; Roberts, J.M.; Tempst, P.; Massague, J. Cloning of p27Kip1, a cyclin-dependent kinase inhibitor and a potential mediator of extracellular antimitogenic signals. *Cell*, **1994**, *78*(1), 59-66.

[80] Kawamata, N.; Morosetti, R.; Miller, C.W.; Park, D.; Spirin, K.S.; Nakamaki, T.; Takeuchi, S.; Hatta, Y.; Simpson, J.; Wilcyznski, S.; *et al.* Molecular analysis of the cyclin-dependent kinase inhibitor gene p27/Kip1 in human malignancies. *Cancer Res*, **1995**, *55*(11), 2266-2269.

[81] Morosetti, R.; Kawamata, N.; Gombart, A.F.; Miller, C.W.; Hatta, Y.; Hirama, T.; Said, J.W.; Tomonaga, M.; Koeffler, H.P. Alterations of the p27KIP1 gene in non-Hodgkin's lymphomas and adult T-cell leukemia/lymphoma. *Blood*, **1995**, *86*(5), 1924-1930.

[82] Shimada, M.; Kitagawa, K.; Dobashi, Y.; Isobe, T.; Hattori, T.; Uchida, C.; Abe, K.; Kotake, Y.; Oda, T.; Suzuki, H.; Hashimoto, K.; Kitagawa, M. High expression of Pirh2, an E3 ligase for p27, is associated with low expression of p27 and poor prognosis in head and neck cancers. *Cancer Sci*, **2009**, *100*(5), 866-872.

[83] Esposito, V.; Baldi, A.; De Luca, A.; Groger, A.M.; Loda, M.; Giordano, G.G.; Caputi, M.; Baldi, F.; Pagano, M.; Giordano, A. Prognostic role of the cyclin-dependent kinase inhibitor p27 in non-small cell lung cancer. *Cancer Res*, **1997**, *57*(16), 3381-3385.

[84] Thomas, G.V.; Szigeti, K.; Murphy, M.; Dractta, G.; Pagano, M.; Loda, M. Down-regulation of p27 is associated with development of colorectal adenocarcinoma metastases. *Am J Pathol*, **1998**, *153*(3), 681-687.

[85] Ciaparrone, M.; Yamamoto, H.; Yao, Y.; Sgambato, A.; Cattoretti, G.; Tomita, N.; Monden, T.; Rotterdam, H.; Weinstein, I.B. Localization and expression of p27KIP1 in multistage colorectal carcinogenesis. *Cancer Res*, **1998**, *58*(1), 114-122.

[86] Carrano, A.C.; Eytan, E.; Hershko, A.; Pagano, M. SKP2 is required for ubiquitin-mediated degradation of the CDK inhibitor p27. *Nat Cell Biol*, **1999**, *1*(4), 193-199.

[87] Gstaiger, M.; Jordan, R.; Lim, M.; Catzavelos, C.; Mestan, J.; Slingerland, J.; Krek, W. Skp2 is oncogenic and overexpressed in human cancers. *Proc Natl Acad Sci U S A*, **2001**, *98*(9), 5043-5048.

[88] Palmqvist, R.; Stenling, R.; Oberg, A.; Landberg, G. Prognostic significance of p27(Kip1) expression in colorectal cancer: a clinico-pathological characterization. *J Pathol*, **1999**, *188*(1), 18-23.

[89] Tan, P.; Cady, B.; Wanner, M.; Worland, P.; Cukor, B.; Magi-Galluzzi, C.; Lavin, P.; Draetta, G.; Pagano, M.; Loda, M. The cell cycle inhibitor p27 is an independent prognostic marker in small (T1a,b) invasive breast carcinomas. *Cancer Res*, **1997**, *57*(7), 1259-1263.

[90] Cote, R.J.; Shi, Y.; Groshen, S.; Feng, A.C.; Cordon-Cardo, C.; Skinner, D.; Lieskovosky, G. Association of p27Kip1 levels with recurrence and survival in patients with stage C prostate carcinoma. *J Natl Cancer Inst*, **1998**, *90*(12), 916-920.

[91] Gerth, J.H.; Kriegsmann, J.; Trinh, T.T.; Stahl, R.A.; Wendt, T.; Sommer, M.; Stein, G.; Wolf, G. Induction of p27KIP1 after unilateral ureteral obstruction is independent of angiotensin II. *Kidney Int*, **2002**, *61*(1), 68-79.

[92] Ophascharoensuk, V.; Fero, M.L.; Hughes, J.; Roberts, J.M.; Shankland, S.J. The cyclin-dependent kinase inhibitor p27Kip1 safeguards against inflammatory injury. *Nat Med*, **1998**, *4*(5), 575-580.

[93] Suzuki, S.; Fukasawa, H.; Kitagawa, K.; Uchida, C.; Hattori, T.; Isobe, T.; Oda, T.; Misaki, T.; Ohashi, N.; Nakayama, K.; Nakayama, K.I.; Hishida, A.; Yamamoto, T.; Kitagawa, M. Renal damage in obstructive nephropathy is decreased in Skp2-deficient mice. *Am J Pathol*, **2007**, *171*(2), 473-483.

[94] Suzuki, S.; Fukasawa, H.; Misaki, T.; Togawa, A.; Ohashi, N.; Kitagawa, K.; Kotake, Y.; Niida, H.; Hishida, A.; Yamamoto, T.; Kitagawa, M. Up-regulation of Cks1 and Skp2 with TNFα/NF-κB Signaling in Chronic Progressive Nephropathy. *Genes to Cells*, **2011**, *in press*.

[95] Ziyadeh, F.N.; Hoffman, B.B.; Han, D.C.; Iglesias-De La Cruz, M.C.; Hong, S.W.; Isono, M.; Chen, S.; McGowan, T.A.; Sharma, K. Long-term prevention of renal insufficiency, excess matrix gene expression, and glomerular mesangial matrix expansion by treatment with monoclonal antitransforming growth factor-beta antibody in db/db diabetic mice. *Proc Natl Acad Sci U S A*, **2000**, *97*(14), 8015-8020.

[96] Fukasawa, H.; Yamamoto, T.; Suzuki, H.; Togawa, A.; Ohashi, N.; Fujigaki, Y.; Uchida, C.; Aoki, M.; Hosono, M.; Kitagawa, M.; Hishida, A. Treatment with anti-TGF-beta antibody ameliorates chronic progressive nephritis by inhibiting Smad/TGF-beta signaling. *Kidney Int*, **2004**, *65*(1), 63-74.

HEPATOLOGY

Hepatitis C Virus NS4B Protein Targets STING and Abrogates RIG-I–Mediated Type I Interferon-Dependent Innate Immunity

Sayuri Nitta,[1*] Naoya Sakamoto,[1,2,6*] Mina Nakagawa,[1,2] Sei Kakinuma,[1,2] Kako Mishima,[1] Akiko Kusano-Kitazume,[1] Kei Kiyohashi,[1] Miyako Murakawa,[1] Yuki Nishimura-Sakurai,[1] Seishin Azuma,[1] Megumi Tasaka-Fujita,[1] Yasuhiro Asahina,[1,2] Mitsutoshi Yoneyama,[3] Takashi Fujita,[4,5] and Mamoru Watanabe[1]

Hepatitis C virus (HCV) infection blocks cellular interferon (IFN)-mediated antiviral signaling through cleavage of Cardif by HCV-NS3/4A serine protease. Like NS3/4A, NS4B protein strongly blocks IFN-β production signaling mediated by retinoic acid–inducible gene I (RIG-I); however, the underlying molecular mechanisms are not well understood. Recently, the stimulator of interferon genes (STING) was identified as an activator of RIG-I signaling. STING possesses a structural homology domain with flaviviral NS4B, which suggests a direct protein-protein interaction. In the present study, we investigated the molecular mechanisms by which NS4B targets RIG-I–induced and STING-mediated IFN-β production signaling. IFN-β promoter reporter assay showed that IFN-β promoter activation induced by RIG-I or Cardif was significantly suppressed by both NS4B and NS3/4A, whereas STING-induced IFN-β activation was suppressed by NS4B but not by NS3/4A, suggesting that NS4B had a distinct point of interaction. Immunostaining showed that STING colocalized with NS4B in the endoplasmic reticulum. Immunoprecipitation and bimolecular fluorescence complementation (BiFC) assays demonstrated that NS4B specifically bound STING. Intriguingly, NS4B expression blocked the protein interaction between STING and Cardif, which is required for robust IFN-β activation. NS4B truncation assays showed that its N terminus, containing the STING homology domain, was necessary for the suppression of IFN-β promoter activation. NS4B suppressed residual IFN-β activation by an NS3/4A-cleaved Cardif (Cardif1-508), suggesting that NS3/4A and NS4B may cooperate in the blockade of IFN-β production. *Conclusion*: NS4B suppresses RIG-I–mediated IFN-β production signaling through a direct protein interaction with STING. Disruption of that interaction may restore cellular antiviral responses and may constitute a novel therapeutic strategy for the eradication of HCV. (HEPATOLOGY 2013;57:46-58)

Type I interferon (IFN) plays a central role in eliminating hepatitis C virus (HCV) both under physiological conditions and when used as a therapeutic intervention.[1-3] In experimental acute-resolving HCV infection in chimpanzees, numerous IFN-related genes are expressed during clinical course of infection.[4] Viruses are recognized by cellular innate immune receptors, such as toll-like receptors, and a family of RIG-I–like receptors, such as retinoic-acid-inducible gene I (RIG-I) and melanoma-differentiation-associated gene 5 (MDA-5); host antiviral responses are then activated, resulting in the

From the [1]Departments of Gastroenterology and Hepatology; [2]Departments of Hepatitis Control, Tokyo Medical and Dental University, Tokyo, Japan; [3]Division of Molecular Immunology, Medical Mycology Research Center, Chiba University, Chiba, Japan; [4]Laboratory of Molecular Genetics, Department of Genetics and Molecular Biology, Institute for Virus Research, Kyoto University, Kyoto, Japan; [5]Laboratory of Molecular Cell Biology, Graduate School of Biostudies, Kyoto University, Kyoto, Japan; and [6]Department of Gastroenterology and Hepatology, Hokkaido University, Hokkaido, Japan.

Received September 16, 2011; accepted July 24, 2012.

BiFC, bimolecular fluorescence complementation; CARD, caspase recruitment domain; DAPI, 4′,6-diamidino-2-phenylindole; dsRNA, double-stranded RNA; ER, endoplasmic reticulum; FACL4, fatty acid-CoA ligase, long chain 4; HCV, hepatitis C virus; IFN, interferon; IKKε, IκB kinase ε; IRF-3, interferon-regulatory factor 3; ISRE, interferon-stimulated response element; MAM, mitochondria-associated ER membrane; mKG, monomeric Kusabira-Green; PDI, protein disulphide-isomerase; pIRF-3, phosphorylated IRF3; poly(dA:dT), poly(deoxyadenylic-deoxythymidylic) acid; RIG-I, retinoic acid–inducible gene I; siRNA, small interfering RNA; SOCS, suppressor of cytokine signaling; STAT1, signal transducer and activator of transcription protein-1; STING, stimulator of interferon genes; TBK1, TANK binding kinase 1.

*These authors contributed equally to this work.

production of cytokines such as type I and type III IFNs.[5] RIG-I is activated through recognition of short double-strand RNA (dsRNA) or triphosphate at the 5′ end of dsRNA as pathogen-associated molecular patterns,[6,7] forming a homo-oligomer that binds with the caspase recruitment domain (CARD) of Cardif (also known as MAVS, VISA, or IPS-1).[8-11] Cardif subsequently recruits TANK binding kinase 1 (TBK1) and IκB kinase ε (IKKε) kinases, which catalyze phosphorylation and activation of IFN regulatory factor-3 (IRF-3).[12] Activation of TBK1 and IKKε results in the phosphorylation of IRF-3 or IRF-7, translocation to the nucleus, and induction of IFN-β mRNA transcription.

Several HCV proteins can block host cellular antiviral responses. HCV core protein blocks IFN signaling by interacting with signal transducer and activator of transcription protein-1 (STAT1).[13] The core protein also induces expression of suppressor of cytokine signaling-1 (SOCS1) and SOCS3, and blocks Janus kinase–STAT signaling.[14,15] A well-elucidated immune evasion strategy of HCV involves NS3/4A serine protease and its ability to inhibit host IFN signal pathways. Gale and colleagues[11,16,17] revealed that NS3/4A protease cleaves Cardif at Cys-508 resulting in dislocation of Cardif from mitochondria, and blocks downstream signaling of IFN-β production. On the other hand, Baril et al.[18] reported that Cardif was still able to form a homo-oligomer and to activate downstream IFN production signaling despite delocalization from the mitochondria. These reports suggest that homo-oligomerization of Cardif, and not mitochondrial anchorage, is essential for the activation of downstream IFN signaling and that other virus-derived molecules may cooperate with NS3/4A to abrogate the signaling of IFN production.

We reported previously that HCV-NS4B, as well as NS3/4A, inhibited RIG-I and Cardif-mediated interferon-stimulated response element (ISRE) activation, while TBK1- and IKKε-mediated ISRE activation were not suppressed.[19] These results indicate that NS4B suppresses IFN production signaling by targeting Cardif or other unknown signaling molecules between the level of Cardif and TBK1/IKKε.

Recently, a stimulator of interferon genes (STING, also known as MITA/ERIS/MPYS/TMEM173) was identified as a positive regulator of RIG-I–mediated IFN-β signaling.[20-23] STING is a 42-kDa protein localized predominantly in the endoplasmic reticulum (ER) that binds RIG-I, Cardif, TBK1, and IKKε. STING is thought to act as a scaffold for Cardif/TBK1/IRF-3 complex upon viral infection.[22] It has been reported that NS4B of yellow fever virus, which is a member of the flaviviridae family of viruses, inhibits STING activation probably through a direct molecular interaction.[24] These reports have led us postulate that HCV-NS4B may also inhibit RIG-I dependent IFN signaling through association with STING.

In the present study, we further investigated the molecular mechanisms by which HCV-NS4B protein inhibits RIG-I–mediated IFN expression signaling. We demonstrated that HCV-NS4B specifically binds STING, blocks the molecular interaction between STING and Cardif, and suppresses the RIG-I–like receptor–induced activation of IFN-β production signaling.

Materials and Methods

Plasmids. The ΔRIG-I and RIG-IKA plasmids express constitutively active and inactive RIG-I, respectively.[5] Full-length Cardif (Cardif) and CARD-truncated Cardif (ΔCARD) plasmids were provided by J. Tschopp.[11] Plasmids expressing STING were provided by G. N. Barber.[20] Plasmids expressing HCV NS3/4A, NS4B, and truncated NS4B have been described.[25] Plasmid pIFNβ-Fluc was provided by R. Lin.[26]

Cell Culture. HEK293T and Huh7 cells were maintained in Dulbecco's modified minimal essential medium (Sigma) supplemented with 2 mM L-glutamine and 10% fetal calf serum at 37°C with 5% CO_2.

HCV Replicon Constructs and HCV-JFH1 Cell Culture. An HCV subgenomic replicon plasmid, pRep-Feo, expressed fusion protein of firefly luciferase and neomycin phosphotransferase.[27,28] Huh7 cells were transfected by Rep-Feo RNA, cultured in the presence of 500 μg/mL of G418, and a cell line that stably expressed Feo replicon was established. For HCV cell culture, the HCV-JFH1 strain was used.[29,30]

Antibodies. Antibodies used were anti–IRF-3 (FL-425, Santa Cruz Biotechnology), anti-HA (Invitrogen), anti-myc (Invitrogen), mouse anti-PDI (Abcam),

Address reprint requests to: Naoya Sakamoto, M.D., Ph.D., Department of Gastroenterology and Hepatology, Hokkaido University, Kita15, Nishi8, Kita-ku, Sapporo, Hokkaido, 060-0808, Japan. E-mail: nsakamoto.gast@tmd.ac.jp; fax (81)-11-706-8036.

View this article online at wileyonlinelibrary.com.

DOI 10.1002/hep.26017

Potential conflict of interest: Nothing to report.

Additional Supporting Information may be found in the online version of this article.

rabbit anti-PDI (Enzo Life Science), anti-Flag (Sigma Aldrich), anti-Cardif (Enzo Life Science), anti-phospho–IRF-3 (Ser396, Millipore), anti-monomeric Kusabira-Green C- or N-terminal fragment (MBL), and anti-FACL4 (Abgent).

Luciferase Reporter Assay. IFN-β reporter assays were performed as described.[19,31] The plasmids pIFN-β-Fluc and pRL-CMV were cotransfected with NS3/4A or NS4B, and ΔRIG-I, Cardif, STING or poly(deoxyadenylic-deoxythymidylic) acid [poly(dA:dT)] (Invivogen). RIG-IKA, ΔCARD, and pcDNA3.1, respectively, were used as controls. Luciferase assays were performed 24 hours after transfection by using a 1420 Multilabel Counter (ARVO MX PerkinElmer) and Dual Luciferase Assay System (Promega). Assays were performed in triplicate, and the results are expressed as the mean ± SD.

Immunoblotting. Preparation of total cell lysates was performed as described.[19,28] Protein was separated using NuPAGE 4%-12% Bis/Tris gels (Invitrogen) and blotted onto an Immobilon polyvinylidene difluoride membrane. The membrane was immunoblotted with primary followed by secondary antibody, and protein was detected by chemiluminescence.

Immunoprecipitation Assay. HEK-293T or Huh7 cells were transfected with plasmids as indicated. Twenty-four hours after transfection, cellular proteins were harvested and immunoprecipitation assays were performed using an Immunoprecipitation Kit according to the manufacturer's protocol (Roche Applied Science). The immunoprecipitated proteins were analyzed by immunoblotting.

Indirect Immunofluorescence Assay. Cells seeded onto tissue culture chamber slides were transfected with plasmids as indicated. Twenty-four hours after transfection, the cells were fixed with cold acetone and incubated with primary antibody and subsequently with Alexa488- or Alexa568-labeled secondary antibodies. Mitochondria were stained by MitoTracker (Invitrogen). Cells were visualized using a confocal laser microscope (Fluoview FV10, Olympus).

BiFC Assay. Expression plasmids of NS4B, Cardif, or STING that was fused with N- or C-terminally truncated monomeric Kusabira-Green (mKG) were constructed by inserting polymerase chain reaction–amplified fragments encoding NS4B, Cardif, or STING, respectively, inserted into fragmented mKG vector (Coral Hue Fluo-Chase Kit; MBL). HEK293T cells were transfected with a complementary pair of mKG fusion plasmids. Twenty-four hours after transfection, fluorescence-positive cells were detected and counted by flow cytometry, or observed by confocal laser microscopy.

Small Interfering RNA Assay. Nucleotide sequences of STING-targeted small interfering RNAs (siRNAs) were as follows: (1) 5′-gcaacagcatctatgagcttctggagaac-3′, (2) 5′- gtgcagtgagccagcggctgtatattctc;-3′, (3) 5′-gctggcat ggtcatattacatcggatatc-3′.[22] Stealth RNAi Negative Control Duplex (Medium GC Duplex, Invitrogen) was used. Forty-eight hours after siRNA transfection, expression levels of STING were detected by immunoblotting.

Statistical Analyses. Statistical analyses were performed using unpaired, two-tailed Student t test. $P < 0.05$ were considered to be statistically significant.

Results

NS4B Suppressed RIG-I, Cardif, and STING-Mediated Activation of IFN-β Expression Signaling. First, we performed a reporter assay using a luciferase reporter plasmid regulated by native IFN-β promoter. Consistent with our previous study,[19] overexpression of NS4B, as well as NS3/4A, inhibited the IFN-β promoter activation that was induced by ΔRIG-I and Cardif, respectively (Fig. 1A). We next studied whether NS4B targets STING and inhibits RIG-I pathway–mediated activation of IFN-β production. Expression of NS4B protein significantly suppressed STING-mediated activation of the IFN-β promoter reporter, whereas expression of NS3/4A showed no effect on STING-induced IFN-β promoter activity (Fig. 1A). To study whether NS4B blocks the STING-mediated DNA-sensing pathway, we performed a reporter assay using a luciferase reporter plasmid cotransfection with poly(dA:dT), which is a synthetic analog of B-DNA and has been reported to induce STING-mediated IFN-β production and NS4B. NS4B significantly blocked poly(dA:dT)-induced IFN-β promoter activation, suggesting that NS4B may block STING signaling in the DNA-sensing pathway (Fig. 1A).

Activation of RIG-I signaling induces phosphorylation of IRF-3, which is a hallmark of IRF-3 activation.[32] Thus, we examined the effects of NS3/4A and NS4B expression on phosphorylation of IRF-3 by immunoblotting analysis. As shown in Fig. 1B, overexpression of ΔRIG-I, Cardif, or STING in HEK293T cells increased levels of phosphorylated IRF-3 (pIRF-3). Expression of NS4B impaired the IRF-3 phosphorylation that was induced by ΔRIG-I, Cardif, or STING. NS3/4A also blocked production of pIRF-3 induced by ΔRIG-I or Cardif. Intriguingly, NS3/4A did not block STING-induced pIRF-3 production. These results demonstrate that both NS3/4A and

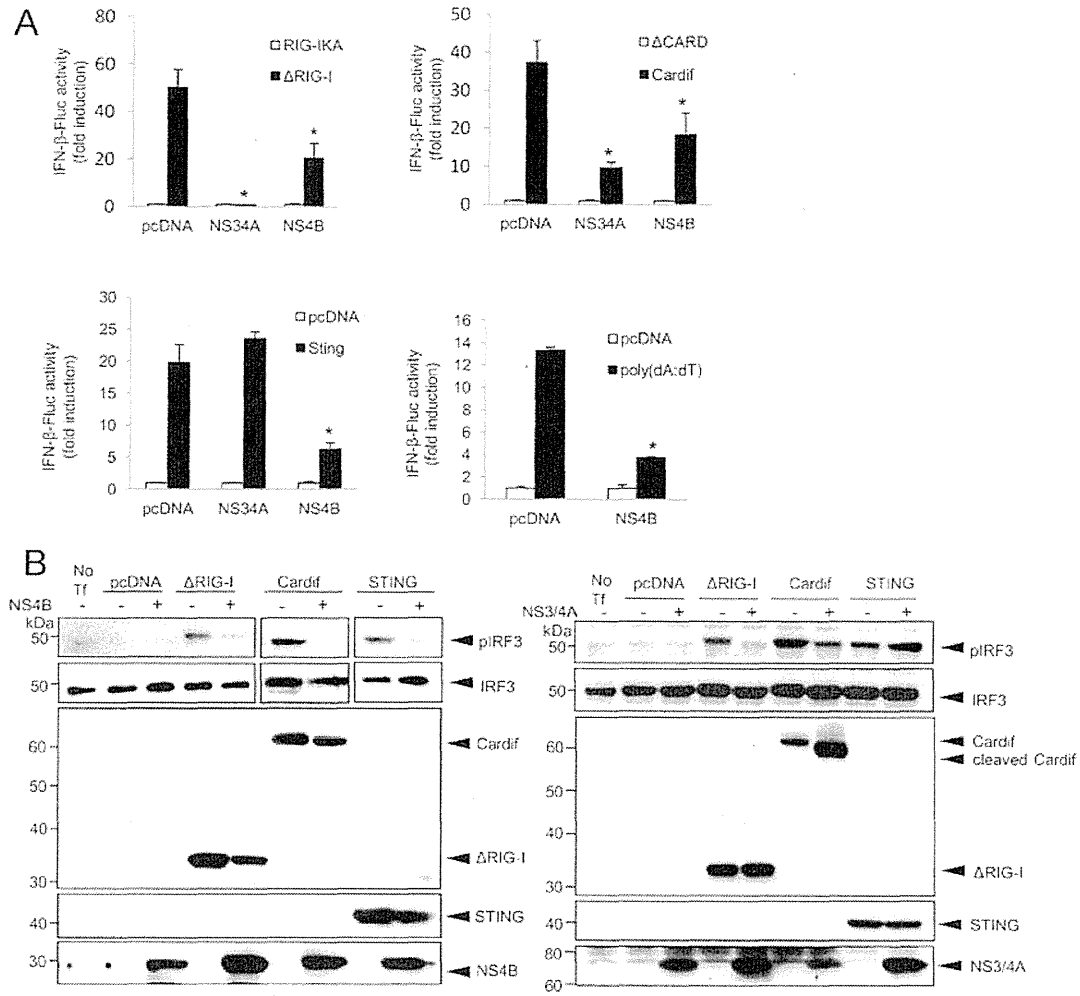

Fig. 1. NS4B suppressed IFN-β signaling mediated by RIG-I, Cardif, or STING. (A) Plasmids expressing ΔRIG-I, Cardif, or STING or poly(dA:dT) as well as NS3/4A or NS4B were cotransfected with pIFN-β-Fluc and pRL-CMV into HEK293T cells. After 24 hours, dual luciferase assays were performed. Plasmids expressing RIG-IKA, ΔCARD, or an empty plasmid (pcDNA) were used as a corresponding negative control. The experiments were performed more than three times and yielded consistent results. The *y* axis indicates relative IFN-β-Fluc activity. Assays were performed in triplicate and error bars indicate mean ± SD. $^*P < 0.05$. (B) HEK293T cells were cotransfected with indicated plasmids. On the day after transfection, the cells were lysed and immunoblot analyses were performed. No Tf, transfection-negative controls. pIRF-3 and IRF-3, phosphorylated and total IRF-3, respectively.

NS4B suppress RIG-I–mediated IFN-β production, but they do so by targeting different molecules in the signaling pathway.

Subcellular Localization of NS4B, Cardif, and STING. We next studied the subcellular localization of NS4B following its overexpression and measured the colocalization of NS4B with Cardif and STING in both HEK293T cells and Huh7 cells by indirect immunofluorescence microscopy. NS4B was localized predominantly in the ER, which is consistent with previous reports[33] (Fig. 2A). Cardif was localized in mitochondria but did not colocalize with the ER-resident host protein disulphide-isomerase (PDI). Interestingly, Cardif and NS4B colocalized partly at the boundary of the two proteins, although their original localization was different (Fig. 2A,C). STING was localized predominantly in the ER[20,21] (Fig. 2B,D). STING colocalized partly with Cardif, which is consistent with a previous report by Ishikawa and Barber[20] (Fig. 2B,D). In cells cotransfected with NS4B and STING expression plasmids, NS4B colocalized precisely with STING (Fig. 2B,D). To examine the region of NS4B-STING interaction, we next observed the two proteins by performing staining for them along with mitochondria-associated ER membrane (MAM), which is a physical association with mitochondria[34] and has been reported the site of Cardif-STING association.[24] Both NS4B and STING were adjacent to and partially colocalized

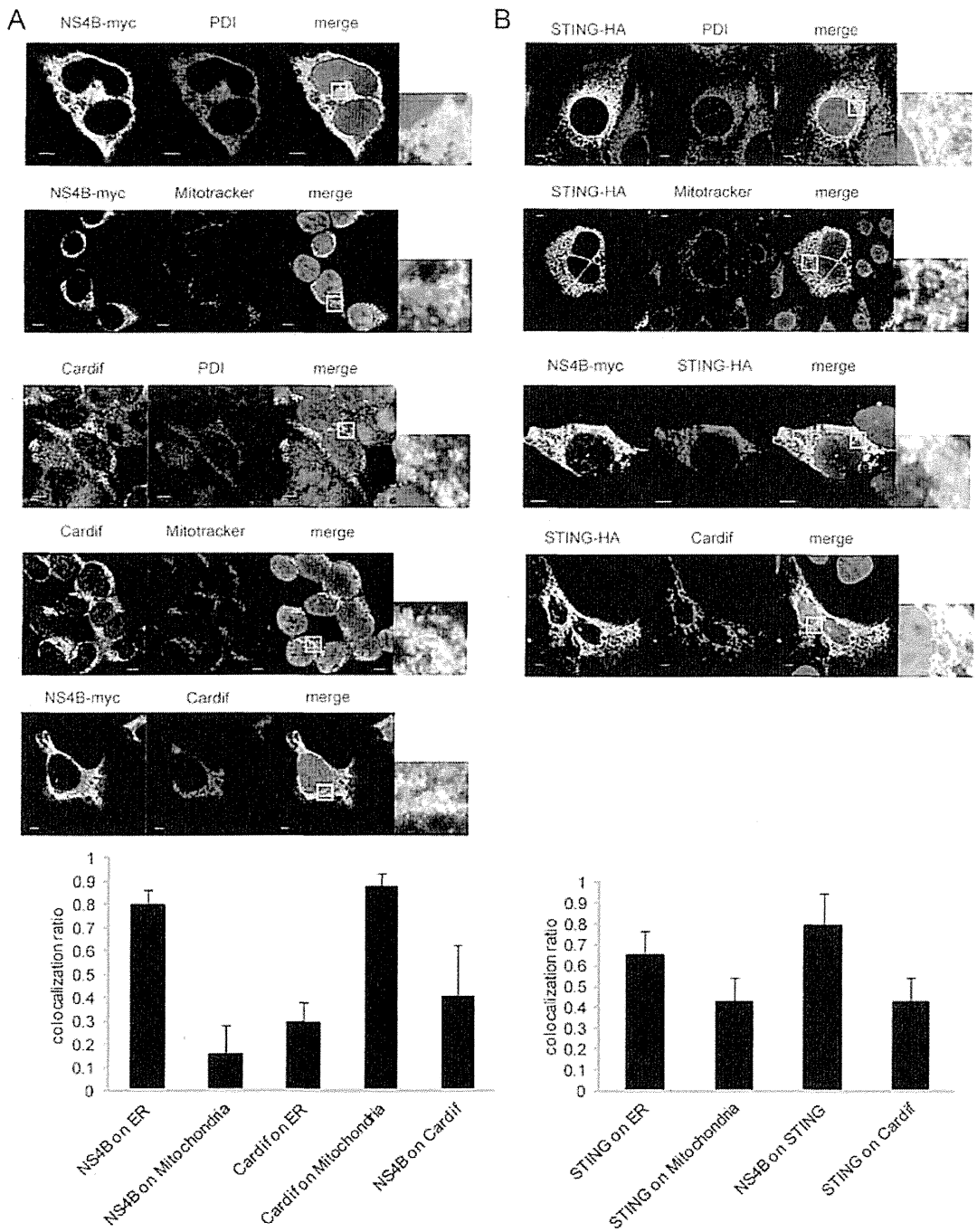

Fig. 2. Subcellular localization of NS4B, Cardif, and STING. (A-D) Subcellular localization of NS4B, Cardif, and STING in 293T (A,C) and Huh7 (B,D) cells. (A,C) NS4B-myc (first, second, and fifth panels of A and third panel of C) was transfected, and 24 hours later the cells were fixed and immunostained with anti-myc. In the third, fourth, and fifth panels of A, and the first and second panels of C, endogenous Cardif was detected with anti-Cardif antibody. ER was immunostained with anti-PDI antibody (first and third panels of A and first panel of C). Mitochondria were stained using Mitotracker (second and fourth panels of A and second panel of C). Nuclei were stained with 4',6-diamidino-2-phenylindole (DAPI). (B,D) STING-HA (all panels) and NS4B-myc (third panels) were transfected, and after 24 hours the cells were fixed and immunostained with anti-HA or anti-myc, respectively. In the fourth panels, endogenous Cardif was detected with anti-Cardif antibody. ER was immunostained with anti-PDI antibody (first panels). Mitochondria were stained using Mitotracker (second panels). Nuclei were stained with DAPI. (E) NS4B-myc and STING-HA were transfected into Huh7 cells and after 24 hours the cells were fixed and immunostained with anti-HA, anti-myc, and anti-FACL4 (MAM) antibody. Cells were visualized by confocal microscopy. Scale bars indicate 5 μm. In each microscopic image, the grade of protein colocalization in a single cell was quantified and is shown in the graphs at the bottom of each panel. Values are shown as the average colocalization ratio in 8 cells. Error bars indicate the mean + SD.

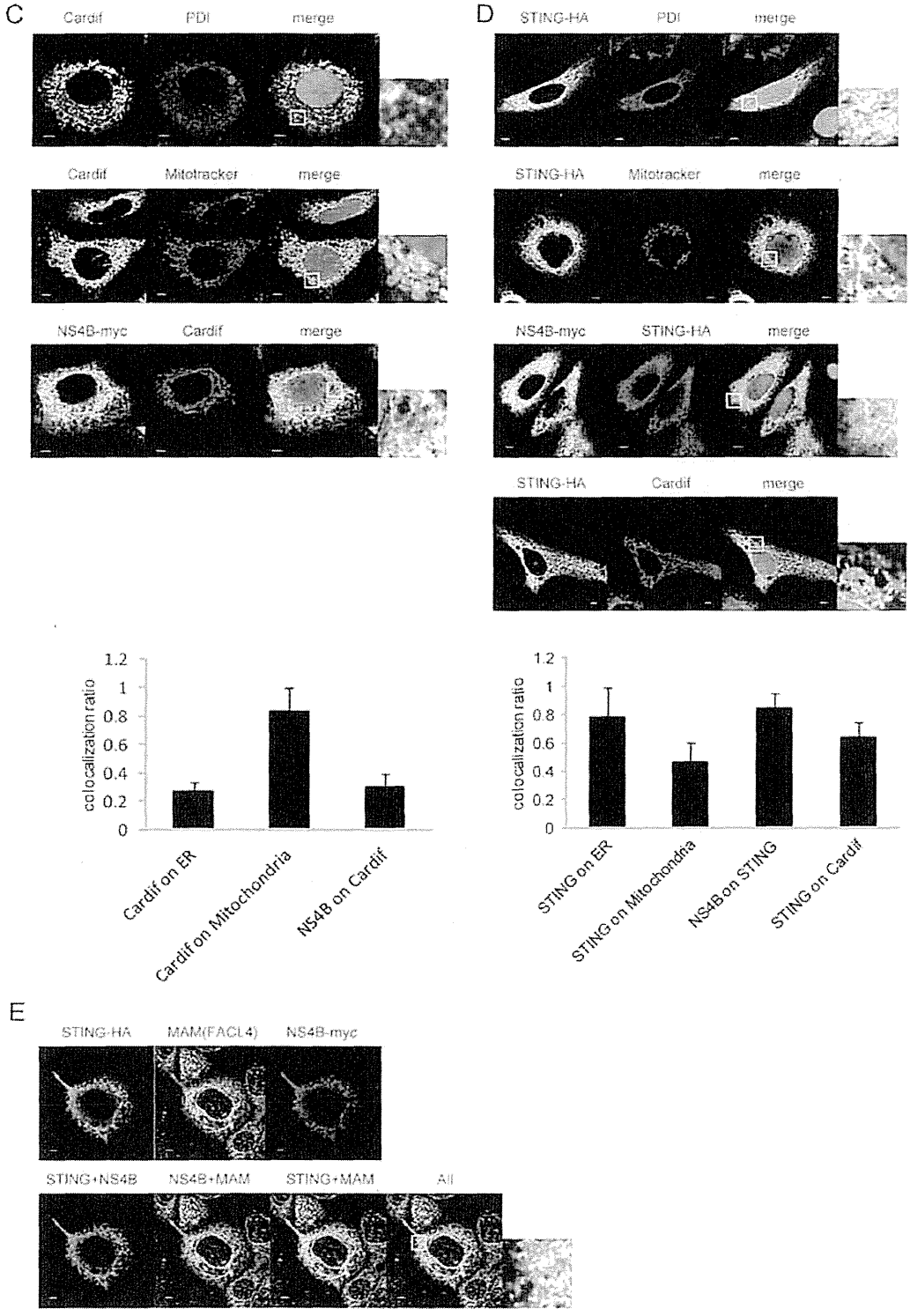

Fig. 2. Continued

with fatty acid-CoA ligase long chain 4 (FACL4), which is a MAM marker protein[35,36] (Fig. 2E). These findings suggest that NS4B might interact with STING on MAM more strongly than with Cardif.

Protein-Protein Interaction Between NS4B, Cardif, and STING. Knowing that NS4B was colocalized strongly with STING and only partly with Cardif, we next analyzed direct protein-protein interactions

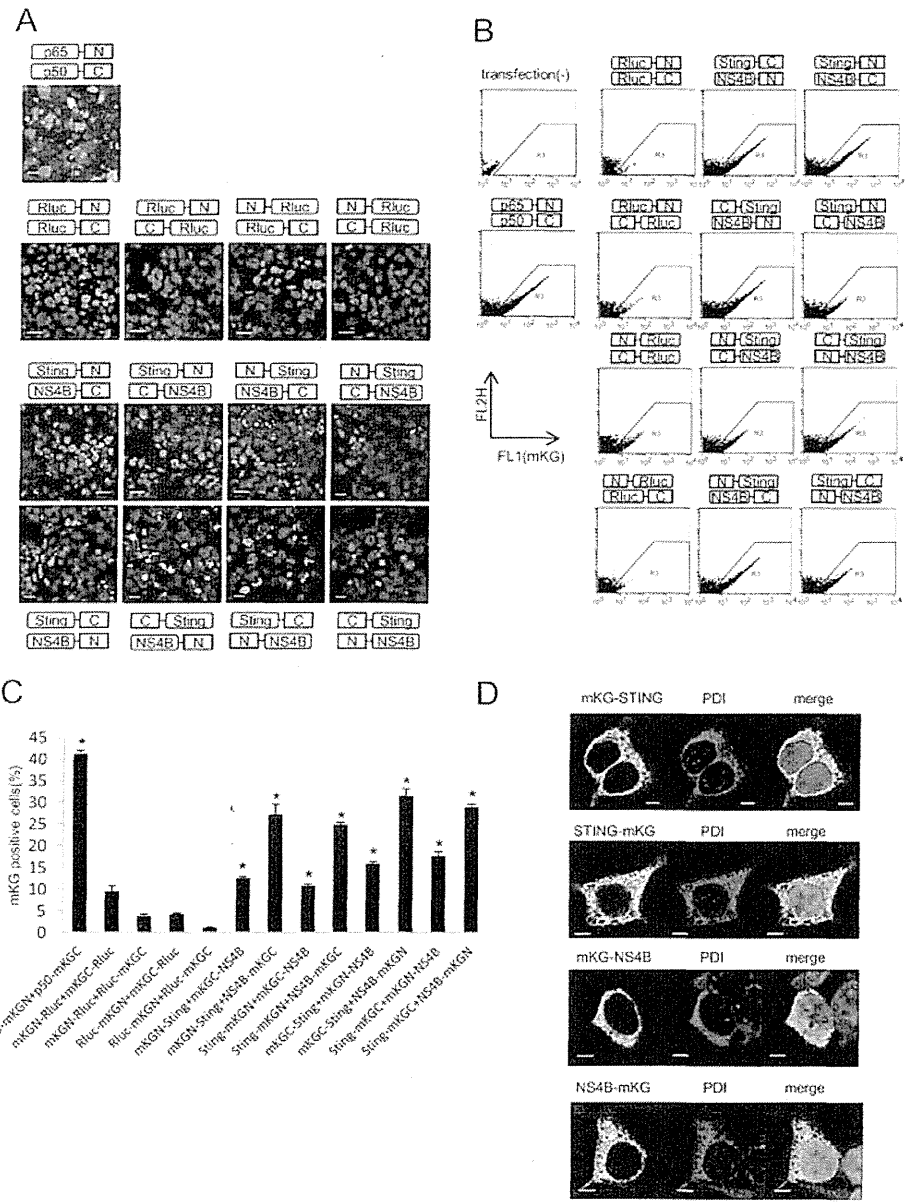

Fig. 3. BiFC assays of STING and NS4B. The complementary pairs of N- or C-terminally mKG-fused NS4B and STING expression plasmids were cotransfected in HEK293T cells. After 24 hours, the cells were fixed and observed by confocal microscopy (A) or subjected to flow cytometry to measure mKG-emitted fluorescence (BiFC signal) and to count BiFC signal-positive cells (B,C). Plasmids expressing p65-mKGN and p50-mKGC individually were used as a BiFC-positive control and plasmids expressing N- or C-terminally mKG fused Rluc were used as a negative control. The letters N and C denote complimentary N- and C-terminal fragments of mKG, respectively. Assays were performed in triplicate and error bars indicate the mean ± SD. Scale bars indicate 10 μm (A). *$P < 0.05$ compared with corresponding negative controls. (D) Plasmids expressing mKG fragment-fused STING or NS4B were transfected in HEK293T cells. After 24 hours, the cells were fixed and immunostained with anti-mKG and anti-PDI (ER) antibody. Nuclei were stained with DAPI. Cells were observed by confocal microscopy. Scale bars = 5 μm.

between NS4B, Cardif, and STING. To detect those interactions in living cells, we performed BiFC assays.[37,38] We constructed NS4B, Cardif, and STING expression plasmids that were N- or C-terminally fused with truncated mKG proteins, respectively. First, we cotransfected several different pairs of NS4B and STING expression plasmids that were fused with complementary pairs of N- or C-terminally truncated mKG. Strong fluorescence by mKG complexes (BiFC signal) was detected in all pairs of cotransfections, suggesting significant molecular interaction (Fig. 3A). In flow cytometry, all pairs of NS4B- and STING-mKG fusion proteins were positive for strong BiFC signal (Fig. 3B). The percentages of cells positive for BiFC signal were significantly higher in STING-mKG and NS4B-mKG fusion complexes than in corresponding controls (Fig. 3C). These results demonstrate that HCV-NS4B and STING proteins interact with each other strongly and specifically in cells. Fluorescence microscopy indicated that N- and C-terminal fusion of mKG onto NS4B and STING did not affect subcellular localization (Fig. 3D).

We next studied the molecular interaction between NS4B and Cardif by BiFC assay using NS4B and Cardif fusion plasmids that were tagged with complementary pairs of truncated mKG. Weak fluorescence was detected in cells transfected with the pairs N-Cardif and NS4B-C, N-Cardif and C-NS4B, C-Cardif and

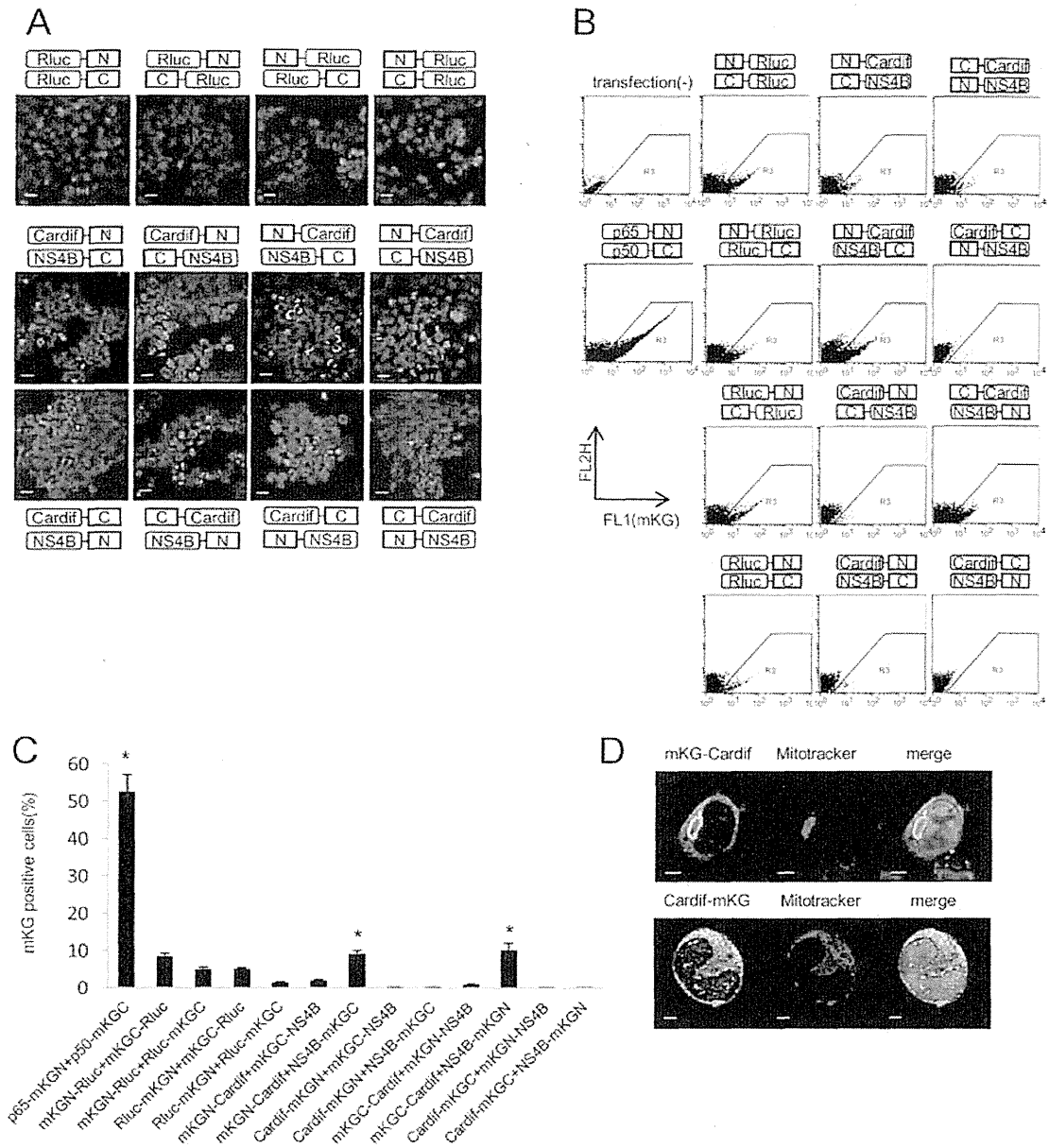

Fig. 4. BiFC assays of Cardif and NS4B. The complementary pairs of N- or C-terminally mKG-fused NS4B and Cardif expression plasmids were cotransfected in HEK293T cells. After 24 hours, the cells were fixed and observed by confocal microscopy (A) or subjected to flow cytometry to measure mKG-emitted fluorescence (BiFC signal) and to count BiFC signal-positive cells (B,C). Plasmids expressing p65-mKGN and p50-mKGC individually were used as a BiFC-positive control and plasmids expressing N- or C-terminally mKG-fused Rluc were used as a negative control. The letters N and C denote complimentary N- and C-terminal fragments of mKG, respectively. Assays were performed in triplicate, and error bars indicate the mean ± SD. Scale bars indicate 10 μm (A). *$P < 0.05$ compared with corresponding negative controls. (D) Plasmids expressing mKG fragment-fused STING or NS4B were transfected in HEK293T cells. After 24 hours, the cells were fixed and immunostained with anti-mKG antibody. Mitochondria were stained using Mitotracker, and nuclei were stained with DAPI. Cells were observed by confocal microscopy. Scale bars = 5 μm.

NS4B-N, and C-Cardif and N-NS4B (Fig. 4A,B). The percentage of cells positive for BiFC signal increased with the combination of N-Cardif and NS4B-C, and C-Cardif and NS4B-N (Fig. 4C). Fluorescence microscopy indicated that mKG-Cardif, but not Cardif-mKG, was partially colocalized with mitochondria, possibly due to disruption of mitochondria anchor domain by C-terminal fusion with mKG (Fig. 4D). These results indicate the lack of significant molecular interactions between NS4B and Cardif.

Binding of NS4B to STING Blocks Molecular Interaction Between Cardif and STING. It has been reported that STING binds Cardif directly.[20,22] Thus, we hypothesized that NS4B, through a competitive